

Finite Difference Approximation with ADI Scheme for Two-dimensional Keller-Segel Equations

Yubin Lu, Chi-An Chen, Xiaofan Li*, Chun Liu

Department of Applied Mathematics, College of Computing, Illinois Institute of Technology, Chicago, IL 60616, USA

Abstract. Keller-Segel systems are a set of nonlinear partial differential equations used to model chemotaxis in biology. In this paper, we propose two alternating direction implicit (ADI) schemes to solve the 2D Keller-Segel systems directly with minimal computational cost, while preserving positivity, energy dissipation law and mass conservation. One scheme unconditionally preserves positivity, while the other does so conditionally. Both schemes achieve second-order accuracy in space, with the former being first-order accuracy in time and the latter second-order accuracy in time. Besides, the former scheme preserves the energy dissipation law asymptotically. We validate these results through numerical experiments, and also compare the efficiency of our schemes with the standard five-point scheme, demonstrating that our approaches effectively reduce computational costs.

AMS subject classifications: 65M06, 35K61, 35K55, 65Z05

Key words: Keller-Segel equations, energy dissipation, positive preserving, ADI scheme.

1 Introduction

The Keller-Segel system as a mathematical model was proposed to model the phenomenon of chemotaxis in biology, established by Patlak [26] and Keller and Segel [17, 18]. Chemotaxis is the migration of organisms in response to chemical signals. Usually, the organisms are attracted by chemical signals that could be emitted by themselves. On the other hand, there is another hidden mechanism, namely the diffusion phenomenon. These two mechanisms compete with each other, leading to different interesting biological phenomena. These phenomena could be summarized by the Keller-Segel equations, a system of parabolic-parabolic equations or parabolic-elliptic equations in a limiting case. So far, the Keller-Segel equations are not limited to describing such biological processes, but can also be widely used to describe various phenomena in social sciences and other competitive systems.

*Corresponding author. *Email address:* lix@iit.edu (X. Li)

One of the most important mathematical issues of the Keller-Segel system is the well-posedness of their solutions. This issue has been well studied by mathematicians in some sense [2, 4, 14, 15]. Roughly speaking, if the initial mass is less than a critical value, the solution exists globally, otherwise the solution will blow up in finite time. Certainly, blow-up does not occur in real scenarios. This indicates that the classical Keller-Segel model has limitations. Therefore, several improved models are designed to relax such restrictions [27]. We will focus on the classical one.

In addition to the analytic aspect of the Keller-Segel equations, the numerical aspect is also extremely important for real applications. The Keller-Segel system consists of two equations, one of which describes the evolution of density of organisms and the other describes the evolution of the chemoattractant concentration. Naturally, the density and the concentration should remain nonnegative, the density should also preserve mass conservation under suitable boundary conditions, and the energy dissipation law holds. A question arises: how do we design numerical solvers that preserve these properties? In addressing this question, many works have been proposed to solve such type equations with specific conditions. The most popular methods including linear/nonlinear finite volume schemes [1, 3, 5, 6, 19, 34], discontinuous Galerkin schemes [10, 20], discontinuous finite element scheme [9], finite difference scheme [25], spectral method [28], and others [8, 16]. Moreover, several general ways have been proposed to preserve the energy dissipation law for specific problems, including scalar auxiliary variable approach (SAV) [30], convex splitting method [7], stabilization method [31, 35], and the method of invariant energy quadratization (IEQ) [32, 33]. Furthermore, numerous numerical schemes have been developed to address the challenges posed by the Poisson-Nernst-Planck equations. Given the interrelated nature of Keller-Segel equations and Poisson-Nernst-Planck equations in the context of numerical scheme design, we recommend that readers consult [21, 23, 24, 29], and the references cited therein for more insights. Although these numerical methods are developed to preserve positivity, mass conservation and energy dissipation and so on, very few of the existing papers take into account the reduction of computational cost while still preserving these desired properties.

In this work, we consider the following 2D Keller-Segel equations

$$\partial_t \rho = \Delta \rho - \nabla \cdot (\rho \nabla c), \quad (1.1)$$

$$\varepsilon \partial_t c = \Delta c + \rho, \quad (1.2)$$

$$\rho(\mathbf{x}, 0) = f(\mathbf{x}), \quad c(\mathbf{x}, 0) = g(\mathbf{x}),$$

where ρ and c are the cell density and the chemoattractant concentration respectively, $\mathbf{x} = (x, y) \in \Omega \subset \mathbb{R}^2$, and ε is a nonnegative constant. To preserve positivity, Liu *et al.* [25] reformulated the density equation (1.1) as the following symmetric form:

$$\partial_t \rho = \nabla \cdot \left(e^c \nabla \left(\frac{\rho}{e^c} \right) \right), \quad (1.3)$$

and proposed the following first-order semi-discrete scheme:

$$\frac{\rho^{n+1} - \rho^n}{\Delta t} = \Delta \rho^{n+1} - \nabla \cdot (\rho^{n+1} \nabla c^{n+1}), \quad (1.4)$$

$$\varepsilon \frac{c^{n+1} - c^n}{\Delta t} = \Delta c^{n+1} + \rho^n. \quad (1.5)$$

This scheme is not only stable, but also preserves positivity and mass conservation under some suitable conditions. See [25] for more details.

It is not hard to realize that naive spatial discretizations of (1.4) might destroy the positivity of the solution and trigger instability. Denoting $M^{n+1} = e^{c^{n+1}}$, Liu *et al.* [25] rewrote the semi-discrete scheme (1.4) based on the symmetric form of the density equation (1.3):

$$\frac{\rho^{n+1} - \rho^n}{\Delta t} = \nabla \cdot \left(M^{n+1} \nabla \left(\frac{\rho^{n+1}}{M^{n+1}} \right) \right), \quad (1.6)$$

$$\varepsilon \frac{c^{n+1} - c^n}{\Delta t} = \Delta c^{n+1} + \rho^n. \quad (1.7)$$

Furthermore, denoting $h^{n+1} = \frac{\rho^{n+1}}{\sqrt{M^{n+1}}}$, one can reformulate (1.6) into

$$h^{n+1} - \frac{\Delta t}{\sqrt{M^{n+1}}} \nabla \cdot \left(M^{n+1} \nabla \left(\frac{h^{n+1}}{\sqrt{M^{n+1}}} \right) \right) = \frac{\rho^n}{\sqrt{M^{n+1}}}. \quad (1.8)$$

We provide some finite difference notations here for convenience

$$\Delta_{+t} v(x, y, t) := v(x, y, t + \Delta t) - v(x, y, t), \quad (1.9)$$

$$\delta_x v(x, y, t) := v\left(x + \frac{1}{2} \Delta x, y, t\right) - v\left(x - \frac{1}{2} \Delta x, y, t\right), \quad (1.10)$$

$$\delta_x^2 v(x, y, t) := v(x + \Delta x, y, t) - 2v(x, y, t) + v(x - \Delta x, y, t), \quad (1.11)$$

$$\delta_y v(x, y, t) := v\left(x, y + \frac{1}{2} \Delta y, t\right) - v\left(x, y - \frac{1}{2} \Delta y, t\right), \quad (1.12)$$

$$\delta_y^2 v(x, y, t) := v(x, y + \Delta y, t) - 2v(x, y, t) + v(x, y - \Delta y, t), \quad (1.13)$$

$$\tau_x v := \frac{1}{\sqrt{M^{n+1}}} \delta_x \left(M^{n+1} \delta_x \left(\frac{v}{\sqrt{M^{n+1}}} \right) \right), \quad (1.14)$$

$$\tau_y v := \frac{1}{\sqrt{M^{n+1}}} \delta_y \left(M^{n+1} \delta_y \left(\frac{v}{\sqrt{M^{n+1}}} \right) \right), \quad (1.15)$$

$$\bar{\tau}_x v := \frac{1}{\sqrt{M^{n+\frac{1}{2}}}} \delta_x \left(M^{n+\frac{1}{2}} \delta_x \left(\frac{v}{\sqrt{M^{n+\frac{1}{2}}}} \right) \right), \quad (1.16)$$

$$\bar{\tau}_y v := \frac{1}{\sqrt{M^{n+\frac{1}{2}}}} \delta_y \left(M^{n+\frac{1}{2}} \delta_y \left(\frac{v}{\sqrt{M^{n+\frac{1}{2}}}} \right) \right). \quad (1.17)$$

We denote the spatial domain of solutions by $\Omega = [a, b] \times [c, d]$, and the mesh sizes by Δx and Δy in x - and y -directions respectively. We use $c_{i,j}^n$ to denote the numerical solution for $c(x_i, y_j, t_n)$. The other variables could be defined in similar ways.

Applying the standard five-point method for spatial discretization, one can obtain

$$\left(\frac{\varepsilon}{\Delta t} - \frac{1}{(\Delta x)^2} \delta_x^2 - \frac{1}{(\Delta y)^2} \delta_y^2 \right) c_{i,j}^{n+1} = \frac{\varepsilon}{\Delta t} c_{i,j}^n + \rho_{i,j}^n, \quad (1.18)$$

$$\left(1 - \frac{\Delta t}{(\Delta x)^2} \tau_x - \frac{\Delta t}{(\Delta y)^2} \tau_y \right) h_{i,j}^{n+1} = \frac{\rho_{i,j}^n}{\sqrt{M_{i,j}^{n+1}}}. \quad (1.19)$$

At n -th time step, one solves a sparse, $N_x N_y \times N_x N_y$ linear system for c^{n+1} from (1.18); then solves another sparse, $N_x N_y \times N_x N_y$ linear system for h^{n+1} from (1.19). Subsequently, we can obtain the density $\rho_{i,j}^{n+1}$ using the following formula:

$$\rho_{i,j}^{n+1} = h_{i,j}^{n+1} \sqrt{M_{i,j}^{n+1}}. \quad (1.20)$$

This scheme not only preserves positivity and mass conservation but also decouples a nonlinear system into a two-stage linear system. This means that the Keller-Segel system could be solved efficiently using iterative methods. However, such as in [25], if the grid is sufficiently fine, the computational cost becomes high. Especially, the solution to the Keller-Segel system blows up in finite time when the initial mass is large than a critical value [27]. In this case, usually, we would have to use an extremely fine grids to capture more precise asymptotic behavior and seek most efficient scheme to minimize computational cost. In this work, we construct an alternating direction implicit (ADI) scheme so that the linear systems corresponding to the discretized equations corresponding to (1.6) and (1.7) can be solved directly with minimal computational cost while still preserving positivity, mass conservation and energy dissipation law asymptotically.

2 ADI schemes

ADI schemes solve the sparse linear systems using fast direct methods when parabolic partial differential equations are discretized in 2D or higher dimensions. In this section, we propose an ADI scheme for solving the Keller-Segel system (1.1) and (1.2). The scheme preserves positivity, mass conservation and energy dissipation law asymptotically.

2.1 The ADI scheme

Concentration equation. The five-point scheme (1.18) for the semi-discrete scheme (1.5) can be written as follows

$$(1 - \mu_x^\varepsilon \delta_x^2 - \mu_y^\varepsilon \delta_y^2) c_{i,j}^{n+1} = c_{i,j}^n + \frac{\Delta t}{\varepsilon} \rho_{i,j}^n, \quad \text{where} \quad \mu_x^\varepsilon = \frac{\Delta t}{\varepsilon (\Delta x)^2} \quad \text{and} \quad \mu_y^\varepsilon = \frac{\Delta t}{\varepsilon (\Delta y)^2}. \quad (2.1)$$

Instead of (2.1), we propose an ADI scheme discretizing Eq. (1.5) as follows

$$(1 - \mu_x^\varepsilon \delta_x^2)(1 - \mu_y^\varepsilon \delta_y^2) c_{i,j}^{n+1} = c_{i,j}^n + \frac{\Delta t}{\varepsilon} \rho_{i,j}^n, \quad (2.2)$$

which is equivalent to the following 2-step method:

$$(1 - \mu_x^\varepsilon \delta_x^2) c_{i,j}^* = c_{i,j}^n + \frac{\Delta t}{\varepsilon} \rho_{i,j}^n, \quad (2.3)$$

$$(1 - \mu_y^\varepsilon \delta_y^2) c_{i,j}^{n+1} = c_{i,j}^*. \quad (2.4)$$

Density equation. The five-point scheme (1.19) for the density ρ can be rewritten as

$$[1 - (\mu_x \tau_x + \mu_y \tau_y)] h_{i,j}^{n+1} = \frac{\rho_{i,j}^n}{\sqrt{M_{i,j}^{n+1}}}, \quad \text{where} \quad \mu_x = \frac{\Delta t}{(\Delta x)^2}, \mu_y = \frac{\Delta t}{(\Delta y)^2}. \quad (2.5)$$

τ_x and τ_y are operators defined as in (1.14) and (1.15). Instead of (2.5), we consider the following ADI method for the semi-discrete equation (1.4)

$$(1 - \mu_x \tau_x) h_{i,j}^* = \frac{\rho_{i,j}^n}{\sqrt{M_{i,j}^{n+1}}}, \quad (2.6)$$

$$(1 - \mu_y \tau_y) h_{i,j}^{n+1} = h_{i,j}^*. \quad (2.7)$$

The 2-step scheme (2.6) and (2.7) is equivalent to

$$(1 - \mu_x \tau_x)(1 - \mu_y \tau_y) h_{i,j}^{n+1} = \frac{\rho_{i,j}^n}{\sqrt{M_{i,j}^{n+1}}}. \quad (2.8)$$

It is straight forward to verify that the leading-order truncation errors of the ADI scheme (2.2) and (2.8) for Keller-Segel system are the same as the five-point scheme (2.1) and (2.5), i.e., second-order in space and first-order in time. See Appendix B. The stability of this scheme holds if the Keller-Segel equations satisfy a technical condition and a small data condition. See [25] for more details.

2.2 Conservative properties of the ADI scheme

2.2.1 Positivity preservation

Preserving positivity in numerical solutions of the Keller-Segel equations is crucial for obtaining physically meaningful results, as it ensures that the solutions accurately reflect the behavior of the system being modeled. In this subsection, we prove that the ADI schemes (2.2) and (2.8) preserve positivity for the Keller-Segel equations.

Theorem 2.1. *Suppose $\rho_{i,j}^0 \geq 0$, then the ADI scheme (2.8) preserves $\rho_{i,j}^n \geq 0, n \in \mathbb{N}$.*

Proof. In order to prove the ADI scheme (2.8) preserves positivity, it is enough to prove the equivalent form (2.6) and (2.7) preserves positivity. Therefore, we prove the first equation (2.6) preserves positivity. The positivity-preserving property of the second equation (2.7) could be proved in a similar way.

Recalling the fully discrete scheme of the operator τ_x :

$$\begin{aligned} \tau_x h_{i,j}^* &= \frac{1}{\sqrt{M_{i,j}^{n+1}}} \delta_x \left(M_{i,j}^{n+1} \delta_x \left(\frac{h^*}{\sqrt{M^{n+1}}} \right)_{i,j} \right) \\ &= \frac{1}{\sqrt{M_{i,j}^{n+1}}} \left[\sqrt{M_{i,j}^{n+1} M_{i+1,j}^{n+1}} \left(\frac{h_{i+1,j}^*}{\sqrt{M_{i+1,j}^{n+1}}} - \frac{h_{i,j}^*}{\sqrt{M_{i,j}^{n+1}}} \right) - \sqrt{M_{i-1,j}^{n+1} M_{i,j}^{n+1}} \left(\frac{h_{i,j}^*}{\sqrt{M_{i,j}^{n+1}}} - \frac{h_{i-1,j}^*}{\sqrt{M_{i-1,j}^{n+1}}} \right) \right]. \end{aligned} \quad (2.9)$$

Here, $M_{i-\frac{1}{2},j}^{n+1}$ is approximated by its geometric mean $\sqrt{M_{i-1,j}^{n+1} M_{i,j}^{n+1}}$ and similarly for the other terms at half grid points. Therefore, the first equation of the scheme for Eq. (2.6) can be written as:

$$\begin{aligned} h_{i,j}^* &= \frac{\mu_x}{\sqrt{M_{i,j}^{n+1}}} \left[\sqrt{M_{i,j}^{n+1} M_{i+1,j}^{n+1}} \left(\frac{h_{i+1,j}^*}{\sqrt{M_{i+1,j}^{n+1}}} - \frac{h_{i,j}^*}{\sqrt{M_{i,j}^{n+1}}} \right) + \sqrt{M_{i-1,j}^{n+1} M_{i,j}^{n+1}} \left(\frac{h_{i-1,j}^*}{\sqrt{M_{i-1,j}^{n+1}}} - \frac{h_{i,j}^*}{\sqrt{M_{i,j}^{n+1}}} \right) \right] \\ &\quad + \frac{\rho_{i,j}^n}{\sqrt{M_{i,j}^{n+1}}}. \end{aligned} \quad (2.10)$$

Let (k,l) be the indices satisfy $h_{k,l}^* / \sqrt{M_{k,l}^{n+1}} = \min_{i,j} \{h_{i,j}^* / \sqrt{M_{i,j}^{n+1}}\}$. Note that $M_{i,j}^{n+1} \geq 0$ and $\rho_{i,j}^n \geq 0$ for arbitrary i,j , then we conclude $h_{k,l}^* / \sqrt{M_{k,l}^{n+1}} \geq 0$ from (2.10) because both terms in the bracket of RHS of (2.10) are nonnegative. Thus, $\min_{i,j} \{h_{i,j}^* / \sqrt{M_{i,j}^{n+1}}\} \geq 0$ which implies $h_{i,j}^* \geq 0$ for all i,j 's. The second equation of the scheme for the density, Eq. (2.7) could be verified similarly. It means that we have shown the positivity preservation of our ADI scheme for the density ρ . \square

Remark 2.1. Expanding the ADI scheme (2.3) and (2.4) for the chemoattractant concentration c

$$c_{i,j}^* = \mu_x^\varepsilon (c_{i+1,j}^* - 2c_{i,j}^* + c_{i-1,j}^*) + c_{i,j}^n + \frac{\Delta t}{\varepsilon} \rho_{i,j}^n, \quad (2.11)$$

$$c_{i,j}^{n+1} = \mu_y^\varepsilon (c_{i,j+1}^{n+1} - 2c_{i,j}^{n+1} + c_{i,j-1}^{n+1}) + c_{i,j}^*, \quad (2.12)$$

we can show the positivity of concentration $c_{i,j}^n \geq 0$ following the same argument as in the proof of Theorem 2.1.

2.2.2 Conservation of mass

Mass conservation, $\frac{d}{dt} \int_{\Omega} \rho dx = 0$, is another important property of the Keller-Segel equations. Therefore, we hope to preserve this property in the spatial discretization. In order to verify mass conservation of the proposed ADI scheme (2.8), we only need to verify $\sum_{i,j} \sqrt{M_{i,j}^{n+1}} \tau_x h_{i,j}^{n+1} = 0$, $\sum_{i,j} \sqrt{M_{i,j}^{n+1}} \tau_y h_{i,j}^{n+1} = 0$ and $\sum_{i,j} \sqrt{M_{i,j}^{n+1}} \tau_x \tau_y h_{i,j}^{n+1} = 0$ separately. For example, we show that the fully discrete scheme of operator τ_x (1.14) satisfies $\sum_{i,j} \sqrt{M_{i,j}^{n+1}} \tau_x h_{i,j}^{n+1} = 0$. To be specific, taking $M_{i+\frac{1}{2},j}^{n+1}$ to be the geometric mean $\sqrt{M_{i,j}^{n+1} M_{i+1,j}^{n+1}}$, we have

$$\begin{aligned} \tau_x h_{i,j}^{n+1} &= \frac{1}{\sqrt{M_{i,j}^{n+1}}} \left[\sqrt{M_{i+1,j}^{n+1} M_{i,j}^{n+1}} \left(\frac{h_{i+1,j}^{n+1}}{\sqrt{M_{i+1,j}^{n+1}}} - \frac{h_{i,j}^{n+1}}{\sqrt{M_{i,j}^{n+1}}} \right) - \sqrt{M_{i,j}^{n+1} M_{i-1,j}^{n+1}} \left(\frac{h_{i,j}^{n+1}}{\sqrt{M_{i,j}^{n+1}}} - \frac{h_{i-1,j}^{n+1}}{\sqrt{M_{i-1,j}^{n+1}}} \right) \right] \\ &= \frac{1}{\sqrt{M_{i,j}^{n+1}}} \left[\left(\sqrt{M_{i,j}^{n+1}} h_{i+1,j}^{n+1} - \sqrt{M_{i-1,j}^{n+1}} h_{i,j}^{n+1} \right) + \left(\sqrt{M_{i,j}^{n+1}} h_{i-1,j}^{n+1} - \sqrt{M_{i+1,j}^{n+1}} h_{i,j}^{n+1} \right) \right]. \end{aligned} \quad (2.13)$$

Summing over (i,j) of the above equation and assuming periodic boundary condition or other mass-conservative boundary conditions, we get

$$\sum_{i,j} \sqrt{M_{i,j}^{n+1}} \tau_x h_{i,j}^{n+1} = 0. \quad (2.14)$$

Similarly, we can verify that the fully discrete scheme of operators τ_y (1.15) and $\tau_x \tau_y$ (A.3) have mass conservation, i.e.,

$$\sum_{i,j} \sqrt{M_{i,j}^{n+1}} \tau_y h_{i,j}^{n+1} = 0, \quad \sum_{i,j} \sqrt{M_{i,j}^{n+1}} \tau_x \tau_y h_{i,j}^{n+1} = 0. \quad (2.15)$$

Combining them into the scheme of density equation (2.8) and recalling $\rho_{i,j}^{n+1} = \sqrt{M_{i,j}^{n+1}} h_{i,j}^{n+1}$, one can verify that the mass conservation of density variable ρ , that is, $\sum_{i,j} \rho_{i,j}^{n+1} = \sum_{i,j} \rho_{i,j}^n$. We note that the mass conservation of the concentration is $\sum_{i,j} c_{i,j}^{n+1} = \sum_{i,j} c_{i,j}^n + \frac{\Delta t}{\varepsilon} \sum_{i,j} \rho_{i,j}^n$ rather than $\sum_{i,j} c_{i,j}^{n+1} = \sum_{i,j} c_{i,j}^n$, which can be shown in the same manner.

Remark 2.2. Since $0 \leq i \leq N_x$ and $0 \leq j \leq N_y$, we remark that the summation $\sum_{i,j}$ should be replaced by $\sum_{i,j=0}^{N_x-1, N_y-1}$ for periodic boundary conditions or $\sum_{i,j=1}^{N_x-1, N_y-1}$ for Neumann-type boundary conditions.

2.2.3 Energy dissipation

It is well known that the free energy of the Keller-Segel system satisfies an entropy-dissipation law. To be specific, the free energy of the parabolic-parabolic Keller-Segel system (1.1) and (1.2) can be expressed as

$$E(\rho, c) = \int_{\Omega} \left[\rho \log \rho - \rho - \rho c + \frac{1}{2} |\nabla c|^2 \right] d\mathbf{x}, \quad (2.16)$$

and the entropy-dissipation equality

$$\frac{d}{dt} E(t) = - \int_{\Omega} [\rho |\nabla (\log \rho - c)|^2 + \varepsilon |\partial_t c|^2] d\mathbf{x}, \quad (2.17)$$

where the domain $\Omega \subset \mathbb{R}^2$ is bounded.

From the framework of energetic variational approach [13], we can define the flow map $\mathbf{x}(\mathbf{X}, t)$ for the cell density ρ based on the mass conservation law:

$$\begin{cases} \mathbf{u}(\mathbf{x}, t) = \mathbf{x}_t, & t > 0, \\ \mathbf{x}(\mathbf{X}, 0) = \mathbf{X}, \end{cases} \quad (2.18)$$

with \mathbf{x} being the Eulerian coordinates, and \mathbf{X} Lagrangian coordinates. Then the mass conservation law can be written as

$$\rho_t + \nabla \cdot (\rho \mathbf{u}) = 0, \quad (2.19)$$

which implies

$$\rho(\mathbf{x}(\mathbf{X}, t), t) = \frac{\rho_0(\mathbf{X})}{\det \frac{\partial \mathbf{x}}{\partial \mathbf{X}}}. \quad (2.20)$$

With the flow map on ρ , the energy dissipation system (2.17) becomes

$$\frac{d}{dt} E(\rho(\mathbf{x}(\mathbf{X}, t), t), c) = - \int_{\Omega} [\rho |\mathbf{u}|^2 + \varepsilon |\partial_t c|^2] d\mathbf{x} = -2\mathcal{D}, \quad (2.21)$$

where c can be viewed as a fixed given function on the flow map of ρ and the energy dissipation $\mathcal{D}(\mathbf{u}, \partial_t c) := \frac{1}{2} \int_{\Omega} [\rho |\mathbf{u}|^2 + \varepsilon |\partial_t c|^2] d\mathbf{x}$. Now, we may define the action functional $\mathcal{A}(\mathbf{x}) = \int_0^T -E dt$ with respect to \mathbf{x} . According to the force balance law

$$\frac{\delta \mathcal{A}}{\delta \mathbf{x}} = \frac{\delta \mathcal{D}}{\delta \mathbf{x}_t}, \quad (2.22)$$

we can get the first equation (1.1) in the Keller-Segel system. On the other hand, we may define another flow map $\mathbf{x}_1(\mathbf{X}, t)$ for the chemoattractant concentration c which satisfies the transport equation [22]:

$$\partial_t c + \mathbf{u}_1 \cdot \nabla c = 0, \quad (2.23)$$

where (2.23) is equivalent to $c(\mathbf{x}_1(\mathbf{X}, t), t) = c_0(\mathbf{X})$. For this flow map, the energy-dissipation system can be seen as

$$\frac{d}{dt} E(\rho(\mathbf{x}_1, t), c_0(\mathbf{X}), F^{-1} \nabla_{\mathbf{X}} c_0(\mathbf{X})) = -2\tilde{\mathcal{D}}, \quad (2.24)$$

where the Jacobian matrix $F = \frac{\partial \mathbf{x}_1}{\partial \mathbf{X}}$ and $\tilde{\mathcal{D}}(\mathbf{u}, \mathbf{u}_1) := \int_{\Omega} \rho |\mathbf{u}|^2 + \epsilon |\mathbf{u}_1 \cdot \nabla c|^2 dx$.

Now by the force balance law (2.22) with \mathbf{x} replaced by \mathbf{x}_1 , we may obtain the second equation (1.2) of the Keller-Segel system. We refer the reader to [12, 13] for more background knowledge of the energetic variational approach.

In this part, we first prove that the original scheme (1.18) and (1.19) for Keller-Segel equations proposed by Liu *et al.* [25] is energy dissipative. Subsequently, we discuss the energy dissipation law for the ADI scheme (2.2) and (2.8).

To this end, we impose two alternative boundary conditions on the density ρ and the concentration c . One is the periodic boundary conditions for ρ and c . The other is the following Neumann-type boundary conditions

$$M \frac{\partial (\frac{\rho}{M})}{\partial n} = 0 \quad \text{and} \quad \frac{\partial c}{\partial n} = 0, \quad \text{on} \quad \partial \Omega. \quad (2.25)$$

We first summarize the semi-discrete scheme result as the following theorem.

Theorem 2.2. *For the solution to the semi-discrete scheme (1.6) and (1.7), we have the following energy dissipation inequality:*

$$E^{n+1} - E^n \leq -\Delta t \int_{\Omega} \left[\rho^{n+1} |\nabla (\log \rho^{n+1} - c^{n+1})|^2 + \epsilon \left| \frac{c^{n+1} - c^n}{\Delta t} \right|^2 \right] dx, \quad \text{for all } n \geq 0, \quad (2.26)$$

where

$$E^n = E(\rho^n, c^n) = \int_{\Omega} \left[\rho^n \log \rho^n - \rho^n - \rho^n c^n + \frac{1}{2} |\nabla c^n|^2 \right] dx. \quad (2.27)$$

Proof. Using the equality

$$(a-b) \log a = (a \log a - a) - (b \log b - b) + \frac{(a-b)^2}{2\psi}, \quad \psi \in [\min\{a, b\}, \max\{a, b\}], \quad (2.28)$$

we have

$$E^{n+1} - E^n = \int_{\Omega} \left[\rho^{n+1} (\log \rho^{n+1} - 1) - \rho^n (\log \rho^n - 1) \right] - \rho^{n+1} c^{n+1} + \rho^n c^n + \frac{1}{2} (|\nabla c^{n+1}|^2 - |\nabla c^n|^2) dx$$

$$\begin{aligned}
&\leq \int_{\Omega} \left[(\rho^{n+1} - \rho^n) \log \rho^{n+1} - \rho^{n+1} c^{n+1} + \rho^n c^n + \frac{1}{2} (|\nabla c^{n+1}|^2 - |\nabla c^n|^2) \right] d\mathbf{x} \\
&= \int_{\Omega} (\rho^{n+1} - \rho^n) (\log \rho^{n+1} - c^{n+1}) d\mathbf{x} + \int_{\Omega} \frac{1}{2} (|\nabla c^{n+1}|^2 - |\nabla c^n|^2) d\mathbf{x} - \int_{\Omega} \rho^n (c^{n+1} - c^n) d\mathbf{x}.
\end{aligned} \tag{2.29}$$

Using Eq. (1.6), integration by parts and either of the boundary conditions on the variable ρ , from (2.29), we obtain

$$\begin{aligned}
E^{n+1} - E^n &\leq \Delta t \int_{\Omega} \nabla \cdot \left[M^{n+1} \nabla \left(\frac{\rho^{n+1}}{M^{n+1}} \right) \right] (\log \rho^{n+1} - c^{n+1}) d\mathbf{x} + \int_{\Omega} \frac{1}{2} (|\nabla c^{n+1}|^2 - |\nabla c^n|^2) d\mathbf{x} \\
&\quad - \int_{\Omega} \rho^n (c^{n+1} - c^n) d\mathbf{x} \\
&= -\Delta t \int_{\Omega} M^{n+1} \nabla \left(\frac{\rho^{n+1}}{M^{n+1}} \right) \cdot \nabla (\log \rho^{n+1} - c^{n+1}) d\mathbf{x} + \int_{\Omega} \frac{1}{2} (|\nabla c^{n+1}|^2 - |\nabla c^n|^2) d\mathbf{x} \\
&\quad - \int_{\Omega} \rho^n (c^{n+1} - c^n) d\mathbf{x}.
\end{aligned} \tag{2.30}$$

For two arbitrary scalars or vectors α, β , using the equality

$$(\alpha - \beta) \cdot \alpha = \frac{1}{2} (|\alpha|^2 - |\beta|^2 + |\alpha - \beta|^2), \tag{2.31}$$

integration by parts and either of the boundary conditions on the variable c , from (2.30), we have

$$\begin{aligned}
E^{n+1} - E^n &\leq -\Delta t \int_{\Omega} M^{n+1} \nabla \left(\frac{\rho^{n+1}}{M^{n+1}} \right) \cdot \nabla (\log \rho^{n+1} - c^{n+1}) d\mathbf{x} + \int_{\Omega} (\nabla c^{n+1} - \nabla c^n) \cdot \nabla c^{n+1} d\mathbf{x} \\
&\quad - \int_{\Omega} \rho^n (c^{n+1} - c^n) d\mathbf{x} \\
&= -\Delta t \int_{\Omega} M^{n+1} \nabla \left(\frac{\rho^{n+1}}{M^{n+1}} \right) \cdot \nabla (\log \rho^{n+1} - c^{n+1}) d\mathbf{x} - \int_{\Omega} (c^{n+1} - c^n) \Delta c^{n+1} d\mathbf{x} \\
&\quad - \int_{\Omega} \rho^n (c^{n+1} - c^n) d\mathbf{x} \\
&= -\Delta t \int_{\Omega} M^{n+1} \nabla \left(\frac{\rho^{n+1}}{M^{n+1}} \right) \cdot \nabla (\log \rho^{n+1} - c^{n+1}) d\mathbf{x} - \int_{\Omega} (c^{n+1} - c^n) (\Delta c^{n+1} + \rho^n) d\mathbf{x}.
\end{aligned} \tag{2.32}$$

Using Eq. (1.7), from (2.32), we have

$$\begin{aligned}
E^{n+1} - E^n &\leq -\Delta t \int_{\Omega} M^{n+1} \nabla \left(\frac{\rho^{n+1}}{M^{n+1}} \right) \cdot \nabla (\log \rho^{n+1} - c^{n+1}) d\mathbf{x} - \varepsilon \Delta t \int_{\Omega} \left| \frac{c^{n+1} - c^n}{\Delta t} \right|^2 d\mathbf{x} \\
&= -\Delta t \int_{\Omega} \left[\rho^{n+1} \left| \nabla (\log \rho^{n+1} - c^{n+1}) \right|^2 + \varepsilon \left| \frac{c^{n+1} - c^n}{\Delta t} \right|^2 \right] d\mathbf{x}.
\end{aligned} \tag{2.33}$$

For the last equality in (2.33), the identical equation $M\nabla\left(\frac{\rho}{M}\right)=\rho\nabla(\log\rho-c)$ are employed. We have shown the following energy dissipation law for the semi-discrete scheme (1.7) and (1.6): For all $n \geq 0$,

$$E^{n+1} - E^n \leq -\Delta t \int_{\Omega} \left[\rho^{n+1} \left| \nabla(\log\rho^{n+1} - c^{n+1}) \right|^2 + \varepsilon \left| \frac{c^{n+1} - c^n}{\Delta t} \right|^2 \right] d\mathbf{x}. \quad (2.34)$$

□

To prove that the fully discrete five-point finite difference scheme (1.18) and (1.19) preserves a discrete version of the energy dissipation, we state two propositions first. For convenience, we assume the number of grid points $N = N_x = N_y$ and $0 \leq i, j \leq N$. We introduce several different inner products for two scalar functions $f(x, y)$ and $g(x, y)$ as follows

$$\langle f, g \rangle_k := \sum_{i,j=1}^{N-1} f_{i,j} g_{i,j} \Delta x \Delta y, \quad (2.35)$$

$$\langle f, g \rangle_{m_x} := \sum_{i=0, j=1}^{N-1} f_{i+\frac{1}{2}, j} g_{i+\frac{1}{2}, j} \Delta x \Delta y, \quad (2.36)$$

$$\langle f, g \rangle_{m_y} := \sum_{i=1, j=0}^{N-1} f_{i, j+\frac{1}{2}} g_{i, j+\frac{1}{2}} \Delta x \Delta y, \quad (2.37)$$

where $f_{i+\frac{1}{2}, j}$ denotes the value at $(x_i + \frac{1}{2}\Delta x, y_j)$, etc.

For 2D vector-valued functions $\mathbf{u}(x, y) = (u_1(x, y), u_2(x, y))$ and $\mathbf{v}(x, y) = (v_1(x, y), v_2(x, y))$, we define the corresponding inner products as

$$\langle \mathbf{u}, \mathbf{v} \rangle_k := \langle u_1, v_1 \rangle_k + \langle u_2, v_2 \rangle_k, \quad (2.38)$$

$$\langle \mathbf{u}, \mathbf{v} \rangle_m := \langle u_1, v_1 \rangle_{m_x} + \langle u_2, v_2 \rangle_{m_y}. \quad (2.39)$$

Besides, we introduce the discrete gradient operator $\delta = \left(\frac{1}{\Delta x} \delta_x, \frac{1}{\Delta y} \delta_y \right)$.

Similar to Flavell *et al.* [11], we have the following two summation-by-parts formulas.

Proposition 2.1. The following summation-by-parts formula holds

$$\begin{aligned} & \left\langle \frac{\sqrt{M^{n+1}}}{(\Delta x)^2} \tau_x \left(\frac{\rho^{n+1}}{\sqrt{M^{n+1}}} \right) + \frac{\sqrt{M^{n+1}}}{(\Delta y)^2} \tau_y \left(\frac{\rho^{n+1}}{\sqrt{M^{n+1}}} \right), \log\rho^{n+1} - c^{n+1} \right\rangle_k \\ &= - \left\langle M^{n+1} \delta \left(\frac{\rho^{n+1}}{M^{n+1}} \right), \delta(\log\rho^{n+1} - c^{n+1}) \right\rangle_m \\ & \quad - \frac{\Delta y}{\Delta x} \sum_{j=1}^{N-1} \left[M_{\frac{1}{2}, j}^{n+1} \delta_x \left(\frac{\rho}{M} \right)_{\frac{1}{2}, j}^{n+1} \left(\log\rho_{0, j}^{n+1} - c_{0, j}^{n+1} \right) \right] \end{aligned}$$

$$\begin{aligned}
& + \frac{\Delta y}{\Delta x} \sum_{j=1}^{N-1} \left[M_{N-\frac{1}{2},j}^{n+1} \delta_x \left(\frac{\rho}{M} \right)_{N-\frac{1}{2},j}^{n+1} \left(\log \rho_{N,j}^{n+1} - c_{N,j}^{n+1} \right) \right] \\
& - \frac{\Delta x}{\Delta y} \sum_{i=1}^{N-1} \left[M_{i,\frac{1}{2}}^{n+1} \delta_y \left(\frac{\rho}{M} \right)_{i,\frac{1}{2}}^{n+1} \left(\log \rho_{i,0}^{n+1} - c_{i,0}^{n+1} \right) \right] \\
& + \frac{\Delta x}{\Delta y} \sum_{i=1}^{N-1} \left[M_{i,N-\frac{1}{2}}^{n+1} \delta_y \left(\frac{\rho}{M} \right)_{i,N-\frac{1}{2}}^{n+1} \left(\log \rho_{i,N}^{n+1} - c_{i,N}^{n+1} \right) \right]. \tag{2.40}
\end{aligned}$$

Furthermore, implementing the Neumann-type boundary conditions (2.25) as $\delta_x \left(\frac{\rho}{M} \right)_{\frac{1}{2},j}^{n+1} = \delta_x \left(\frac{\rho}{M} \right)_{N-\frac{1}{2},j}^{n+1} = \delta_y \left(\frac{\rho}{M} \right)_{i,\frac{1}{2}}^{n+1} = \delta_y \left(\frac{\rho}{M} \right)_{i,N-\frac{1}{2}}^{n+1} = 0$, we obtain the following simplified version of summation-by-parts formula

$$\begin{aligned}
& \left\langle \frac{\sqrt{M^{n+1}}}{(\Delta x)^2} \tau_x \left(\frac{\rho^{n+1}}{\sqrt{M^{n+1}}} \right) + \frac{\sqrt{M^{n+1}}}{(\Delta y)^2} \tau_y \left(\frac{\rho^{n+1}}{\sqrt{M^{n+1}}} \right), \log \rho^{n+1} - c^{n+1} \right\rangle_k \\
& = - \left\langle M^{n+1} \delta \left(\frac{\rho^{n+1}}{M^{n+1}} \right), \delta \left(\log \rho^{n+1} - c^{n+1} \right) \right\rangle_m. \tag{2.41}
\end{aligned}$$

Proof. By the definition, we have

$$\begin{aligned}
& \left\langle \frac{\sqrt{M^{n+1}}}{(\Delta x)^2} \tau_x \left(\frac{\rho^{n+1}}{\sqrt{M^{n+1}}} \right) + \frac{\sqrt{M^{n+1}}}{(\Delta y)^2} \tau_y \left(\frac{\rho^{n+1}}{\sqrt{M^{n+1}}} \right), \log \rho^{n+1} - c^{n+1} \right\rangle_k \\
& = \Delta x \Delta y \sum_{i,j=1}^{N-1} \left\{ \frac{1}{(\Delta x)^2} \delta_x \left[M^{n+1} \delta_x \left(\frac{\rho^{n+1}}{M^{n+1}} \right) \right]_{i,j} + \frac{1}{(\Delta y)^2} \delta_y \left[M^{n+1} \delta_y \left(\frac{\rho^{n+1}}{M^{n+1}} \right) \right]_{i,j} \right\} \left(\log \rho_{i,j}^{n+1} - c_{i,j}^{n+1} \right) \\
& = \Delta y \sum_{i,j=1}^{N-1} \left[\frac{M_{i+\frac{1}{2},j}^{n+1} \delta_x \left(\frac{\rho}{M} \right)_{i+\frac{1}{2},j}^{n+1} - M_{i-\frac{1}{2},j}^{n+1} \delta_x \left(\frac{\rho}{M} \right)_{i-\frac{1}{2},j}^{n+1}}{\Delta x} \right] \left(\log \rho_{i,j}^{n+1} - c_{i,j}^{n+1} \right) \\
& \quad + \Delta x \sum_{i,j=1}^{N-1} \left[\frac{M_{i,j+\frac{1}{2}}^{n+1} \delta_y \left(\frac{\rho}{M} \right)_{i,j+\frac{1}{2}}^{n+1} - M_{i,j-\frac{1}{2}}^{n+1} \delta_y \left(\frac{\rho}{M} \right)_{i,j-\frac{1}{2}}^{n+1}}{\Delta y} \right] \left(\log \rho_{i,j}^{n+1} - c_{i,j}^{n+1} \right). \tag{2.42}
\end{aligned}$$

For the first term on the right-hand side of (2.42), we can split it into two parts as follows

$$\begin{aligned}
& \Delta y \sum_{i,j=1}^{N-1} \left[\frac{M_{i+\frac{1}{2},j}^{n+1} \delta_x \left(\frac{\rho}{M} \right)_{i+\frac{1}{2},j}^{n+1} - M_{i-\frac{1}{2},j}^{n+1} \delta_x \left(\frac{\rho}{M} \right)_{i-\frac{1}{2},j}^{n+1}}{\Delta x} \right] \left(\log \rho_{i,j}^{n+1} - c_{i,j}^{n+1} \right) \\
& = \frac{\Delta y}{\Delta x} \sum_{i,j=1}^{N-1} \left[M_{i+\frac{1}{2},j}^{n+1} \delta_x \left(\frac{\rho}{M} \right)_{i+\frac{1}{2},j}^{n+1} \left(\log \rho_{i,j}^{n+1} - c_{i,j}^{n+1} \right) \right] \\
& \quad - \frac{\Delta y}{\Delta x} \sum_{i,j=1}^{N-1} \left[M_{i-\frac{1}{2},j}^{n+1} \delta_x \left(\frac{\rho}{M} \right)_{i-\frac{1}{2},j}^{n+1} \left(\log \rho_{i,j}^{n+1} - c_{i,j}^{n+1} \right) \right]
\end{aligned}$$

$$\begin{aligned}
&= \frac{\Delta y}{\Delta x} \sum_{i,j=1}^{N-1} \left[M_{i+\frac{1}{2},j}^{n+1} \delta_x \left(\frac{\rho}{M} \right)_{i+\frac{1}{2},j}^{n+1} \left(\log \rho_{i,j}^{n+1} - c_{i,j}^{n+1} \right) \right] \\
&\quad - \frac{\Delta y}{\Delta x} \sum_{i=0}^{N-2} \sum_{j=1}^{N-1} \left[M_{i+\frac{1}{2},j}^{n+1} \delta_x \left(\frac{\rho}{M} \right)_{i+\frac{1}{2},j}^{n+1} \left(\log \rho_{i+1,j}^{n+1} - c_{i+1,j}^{n+1} \right) \right] \\
&= -\Delta x \Delta y \sum_{i=0,j=1}^{N-1} \left[M_{i+\frac{1}{2},j}^{n+1} \frac{\delta_x \left(\frac{\rho}{M} \right)_{i+\frac{1}{2},j}^{n+1} \left(\log \rho_{i+1,j}^{n+1} - c_{i+1,j}^{n+1} \right) - \left(\log \rho_{i,j}^{n+1} - c_{i,j}^{n+1} \right)}{\Delta x} \right] \\
&\quad - \frac{\Delta y}{\Delta x} \sum_{j=1}^{N-1} \left[M_{\frac{1}{2},j}^{n+1} \delta_x \left(\frac{\rho}{M} \right)_{\frac{1}{2},j}^{n+1} \left(\log \rho_{0,j}^{n+1} - c_{0,j}^{n+1} \right) \right] \\
&\quad + \frac{\Delta y}{\Delta x} \sum_{j=1}^{N-1} \left[M_{N-\frac{1}{2},j}^{n+1} \delta_x \left(\frac{\rho}{M} \right)_{N-\frac{1}{2},j}^{n+1} \left(\log \rho_{N,j}^{n+1} - c_{N,j}^{n+1} \right) \right] \\
&= -\frac{1}{(\Delta x)^2} \left\langle M^{n+1} \delta_x \left(\frac{\rho^{n+1}}{M^{n+1}} \right), \delta_x \left(\log \rho^{n+1} - c^{n+1} \right) \right\rangle_{m_x} \\
&\quad - \frac{\Delta y}{\Delta x} \sum_{j=1}^{N-1} \left[M_{\frac{1}{2},j}^{n+1} \delta_x \left(\frac{\rho}{M} \right)_{\frac{1}{2},j}^{n+1} \left(\log \rho_{0,j}^{n+1} - c_{0,j}^{n+1} \right) \right] \\
&\quad + \frac{\Delta y}{\Delta x} \sum_{j=1}^{N-1} \left[M_{N-\frac{1}{2},j}^{n+1} \delta_x \left(\frac{\rho}{M} \right)_{N-\frac{1}{2},j}^{n+1} \left(\log \rho_{N,j}^{n+1} - c_{N,j}^{n+1} \right) \right]. \tag{2.43}
\end{aligned}$$

Similarly, for the second term on the right-hand side of (2.42), we have

$$\begin{aligned}
&\Delta x \sum_{i,j=1}^{N-1} \left[\frac{M_{i,j+\frac{1}{2}}^{n+1} \delta_y \left(\frac{\rho}{M} \right)_{i,j+\frac{1}{2}}^{n+1} - M_{i,j-\frac{1}{2}}^{n+1} \delta_y \left(\frac{\rho}{M} \right)_{i,j-\frac{1}{2}}^{n+1}}{\Delta y} \right] \left(\log \rho_{i,j}^{n+1} - c_{i,j}^{n+1} \right) \\
&= -\frac{1}{(\Delta y)^2} \left\langle M^{n+1} \delta_y \left(\frac{\rho^{n+1}}{M^{n+1}} \right), \delta_y \left(\log \rho^{n+1} - c^{n+1} \right) \right\rangle_{m_y} \\
&\quad - \frac{\Delta x}{\Delta y} \sum_{i=1}^{N-1} \left[M_{i,\frac{1}{2}}^{n+1} \delta_y \left(\frac{\rho}{M} \right)_{i,\frac{1}{2}}^{n+1} \left(\log \rho_{i,0}^{n+1} - c_{i,0}^{n+1} \right) \right] \\
&\quad + \frac{\Delta x}{\Delta y} \sum_{i=1}^{N-1} \left[M_{i,N-\frac{1}{2}}^{n+1} \delta_y \left(\frac{\rho}{M} \right)_{i,N-\frac{1}{2}}^{n+1} \left(\log \rho_{i,N}^{n+1} - c_{i,N}^{n+1} \right) \right]. \tag{2.44}
\end{aligned}$$

Combining (2.43) and (2.44), we obtain the formula (2.40).

If the Neumann-type boundary conditions (2.25) are discretized as $\delta_x \left(\frac{\rho}{M} \right)_{\frac{1}{2},j}^{n+1} = \delta_x \left(\frac{\rho}{M} \right)_{N-\frac{1}{2},j}^{n+1} = \delta_y \left(\frac{\rho}{M} \right)_{i,\frac{1}{2}}^{n+1} = \delta_y \left(\frac{\rho}{M} \right)_{i,N-\frac{1}{2}}^{n+1} = 0$, (2.40) is simplified to (2.41). \square

Remark 2.3. If the boundary conditions is given as periodic conditions, the simplified formula (2.41) holds if we redefine the inner products in (2.35)-(2.37) as

$$\langle f, g \rangle_k := \sum_{i,j=0}^{N-1} f_{i,j} g_{i,j} \Delta x \Delta y, \quad (2.45)$$

$$\langle f, g \rangle_{m_x} := \sum_{i,j=0}^{N-1} f_{i+\frac{1}{2},j} g_{i+\frac{1}{2},j} \Delta x \Delta y, \quad (2.46)$$

$$\langle f, g \rangle_{m_y} := \sum_{i,j=0}^{N-1} f_{i,j+\frac{1}{2}} g_{i,j+\frac{1}{2}} \Delta x \Delta y. \quad (2.47)$$

Similarly, we can also prove the following summation-by-parts formula.

Proposition 2.2.

$$\begin{aligned} \langle c^{n+1} - c^n, \delta^2 c^{n+1} \rangle_k &= - \langle \delta c^{n+1}, \delta (c^{n+1} - c^n) \rangle_m \\ &\quad - \frac{\Delta y}{\Delta x} \sum_{j=1}^{N-1} (c_{0,j}^{n+1} - c_{0,j}^n) \delta_x c_{\frac{1}{2},j}^{n+1} + \frac{\Delta y}{\Delta x} \sum_{j=1}^{N-1} (c_{N,j}^{n+1} - c_{N,j}^n) \delta_x c_{N-\frac{1}{2},j}^{n+1} \\ &\quad - \frac{\Delta x}{\Delta y} \sum_{i=1}^{N-1} (c_{i,0}^{n+1} - c_{i,0}^n) \delta_x c_{i,\frac{1}{2}}^{n+1} + \frac{\Delta x}{\Delta y} \sum_{i=1}^{N-1} (c_{i,N}^{n+1} - c_{i,N}^n) \delta_x c_{i,N-\frac{1}{2}}^{n+1}. \end{aligned} \quad (2.48)$$

Furthermore, implementing the Neumann-type boundary conditions (2.25) as $\delta_x c_{\frac{1}{2},j}^{n+1} = \delta_x c_{N-\frac{1}{2},j}^{n+1} = \delta_y c_{i,\frac{1}{2}}^{n+1} = \delta_y c_{i,N-\frac{1}{2}}^{n+1} = 0$, we have

$$\langle c^{n+1} - c^n, \delta^2 c^{n+1} \rangle_k = - \langle \delta c^{n+1}, \delta (c^{n+1} - c^n) \rangle_m. \quad (2.49)$$

Proof. The proof is similar to that of Proposition 2.1. \square

Remark 2.4. If the boundary conditions is given as periodic conditions, the simplified formula (2.49) holds if we redefine the inner products in (2.35)-(2.37) as Remark 2.3.

Now we are ready to show the discrete version of the energy dissipation law. When the boundary conditions are of Neumann-type, we approximate E^n by the fully discrete energy at time t_n as

$$\mathcal{E}^n = \Delta x \Delta y \sum_{i,j=1}^{N-1} \left[\rho_{i,j}^n \log \rho_{i,j}^n - \rho_{i,j}^n - \rho_{i,j}^n c_{i,j}^n \right] + \frac{1}{2} \Delta x \Delta y \left[\sum_{i=0,j=1}^{N-1} \left| \frac{\delta_x c_{i+\frac{1}{2},j}^n}{\Delta x} \right|^2 + \sum_{i=1,j=0}^{N-1} \left| \frac{\delta_y c_{i,j+\frac{1}{2}}^n}{\Delta y} \right|^2 \right]. \quad (2.50)$$

When the boundary conditions are periodic, we approximate E^n (2.27) as

$$\mathcal{E}^n = \Delta x \Delta y \sum_{i,j=0}^{N-1} \left[\rho_{i,j}^n \log \rho_{i,j}^n - \rho_{i,j}^n - \rho_{i,j}^n c_{i,j}^n \right] + \frac{1}{2} \Delta x \Delta y \left[\sum_{i,j=0}^{N-1} \left| \frac{\delta_x c_{i+\frac{1}{2},j}^n}{\Delta x} \right|^2 + \sum_{i,j=0}^{N-1} \left| \frac{\delta_y c_{i,j+\frac{1}{2}}^n}{\Delta y} \right|^2 \right]. \quad (2.51)$$

Remark 2.5. Under Neumann-type boundary conditions, the discrete energy \mathcal{E}^n (2.50) has the leading order quadratic error $O(\Delta x \Delta y)$ for approximating the analytic energy $E(\rho(t_n), c(t_n))$. Under the periodic boundary conditions, the first term of (2.51) approximates $\int_{\Omega} (\rho^n \log \rho^n - \rho^n - \rho^n c^n) dx$ with spectral accuracy while the second term of (2.51) has the leading-order error of $O((\Delta x)^3 \Delta y) + O(\Delta x (\Delta y)^3)$ due to the second-order accuracy of central differencing $\frac{\delta_x c_{i+\frac{1}{2},j}^n}{\Delta x}$ to $\frac{\partial c}{\partial x}(x_{i+\frac{1}{2}}, y_j, t_n)$ and $\frac{\delta_y c_{i,j+\frac{1}{2}}^n}{\Delta y}$ to $\frac{\partial c}{\partial y}(x_i, y_{j+\frac{1}{2}}, t_n)$.

The following discrete version of the energy dissipation law holds for the finite difference scheme (1.18) and (1.19).

Theorem 2.3. *For the solution to the finite difference scheme (1.18) and (1.19), we have the following energy dissipation inequality:*

$$\begin{aligned} \mathcal{E}^{n+1} - \mathcal{E}^n &\leq -\Delta t \left\langle M^{n+1} \delta \left(\frac{\rho^{n+1}}{M^{n+1}} \right), \delta \left(\log \rho^{n+1} - c^{n+1} \right) \right\rangle_m \\ &\quad - \varepsilon \Delta t \left\langle \frac{c^{n+1} - c^n}{\Delta t}, \frac{c^{n+1} - c^n}{\Delta t} \right\rangle_k. \end{aligned} \quad (2.52)$$

Proof. Using the equality (2.28), we have

$$\begin{aligned} \mathcal{E}^{n+1} - \mathcal{E}^n &= \Delta x \Delta y \sum_{i,j=1}^{N-1} \left[\rho_{i,j}^{n+1} \left(\log \rho_{i,j}^{n+1} - 1 \right) - \rho_{i,j}^n \left(\log \rho_{i,j}^n - 1 \right) \right] \\ &\quad - \Delta x \Delta y \sum_{i,j=1}^{N-1} \left[\rho_{i,j}^{n+1} c_{i,j}^{n+1} - \rho_{i,j}^n c_{i,j}^n \right] \\ &\quad + \frac{1}{2} \frac{\Delta y}{\Delta x} \sum_{i=0,j=1}^{N-1} \left(\left| \delta_x c_{i+\frac{1}{2},j}^{n+1} \right|^2 - \left| \delta_x c_{i+\frac{1}{2},j}^n \right|^2 \right) + \frac{1}{2} \frac{\Delta x}{\Delta y} \sum_{i=1,j=0}^{N-1} \left(\left| \delta_y c_{i,j+\frac{1}{2}}^{n+1} \right|^2 - \left| \delta_y c_{i,j+\frac{1}{2}}^n \right|^2 \right) \\ &\leq \Delta x \Delta y \sum_{i,j=1}^{N-1} \left[\left(\rho_{i,j}^{n+1} - \rho_{i,j}^n \right) \log \rho_{i,j}^{n+1} \right] - \Delta x \Delta y \sum_{i,j=1}^{N-1} \left[\rho_{i,j}^{n+1} c_{i,j}^{n+1} - \rho_{i,j}^n c_{i,j}^n \right] \\ &\quad + \frac{1}{2} \frac{\Delta y}{\Delta x} \sum_{i=0,j=1}^{N-1} \left(\left| \delta_x c_{i+\frac{1}{2},j}^{n+1} \right|^2 - \left| \delta_x c_{i+\frac{1}{2},j}^n \right|^2 \right) + \frac{1}{2} \frac{\Delta x}{\Delta y} \sum_{i=1,j=0}^{N-1} \left(\left| \delta_y c_{i,j+\frac{1}{2}}^{n+1} \right|^2 - \left| \delta_y c_{i,j+\frac{1}{2}}^n \right|^2 \right) \\ &= \Delta x \Delta y \sum_{i,j=1}^{N-1} \left[\left(\rho_{i,j}^{n+1} - \rho_{i,j}^n \right) \left(\log \rho_{i,j}^{n+1} - c_{i,j}^{n+1} \right) - \rho_{i,j}^n \left(c_{i,j}^{n+1} - c_{i,j}^n \right) \right] \end{aligned}$$

$$+ \frac{1}{2} \frac{\Delta y}{\Delta x} \sum_{i=0, j=1}^{N-1} \left(\left| \delta_x c_{i+\frac{1}{2}, j}^{n+1} \right|^2 - \left| \delta_x c_{i+\frac{1}{2}, j}^n \right|^2 \right) + \frac{1}{2} \frac{\Delta x}{\Delta y} \sum_{i=1, j=0}^{N-1} \left(\left| \delta_y c_{i, j+\frac{1}{2}}^{n+1} \right|^2 - \left| \delta_y c_{i, j+\frac{1}{2}}^n \right|^2 \right). \quad (2.53)$$

Using the equality (2.31), from (2.53), we have

$$\begin{aligned} \mathcal{E}^{n+1} - \mathcal{E}^n &\leq \Delta x \Delta y \sum_{i, j=1}^{N-1} \left[\left(\rho_{i, j}^{n+1} - \rho_{i, j}^n \right) \left(\log \rho_{i, j}^{n+1} - c_{i, j}^{n+1} \right) - \rho_{i, j}^n \left(c_{i, j}^{n+1} - c_{i, j}^n \right) \right] \\ &\quad + \frac{\Delta y}{\Delta x} \sum_{i=0, j=1}^{N-1} \left(\delta_x c_{i+\frac{1}{2}, j}^{n+1} - \delta_x c_{i+\frac{1}{2}, j}^n \right) \delta_x c_{i+\frac{1}{2}, j}^{n+1} + \frac{\Delta x}{\Delta y} \sum_{i=1, j=0}^{N-1} \left(\delta_y c_{i, j+\frac{1}{2}}^{n+1} - \delta_y c_{i, j+\frac{1}{2}}^n \right) \delta_y c_{i, j+\frac{1}{2}}^{n+1} \\ &= \left\langle \rho^{n+1} - \rho^n, \log \rho^{n+1} - c^{n+1} \right\rangle_k + \left\langle \frac{\delta_x c^{n+1} - \delta_x c^n}{\Delta x}, \frac{\delta_x c^{n+1}}{\Delta x} \right\rangle_{m_x} \\ &\quad + \left\langle \frac{\delta_y c^{n+1} - \delta_y c^n}{\Delta y}, \frac{\delta_y c^{n+1}}{\Delta y} \right\rangle_{m_y} - \left\langle c^{n+1} - c^n, \rho^n \right\rangle_k. \end{aligned} \quad (2.54)$$

Using Eqs. (1.18)-(1.19), Proposition 2.1, Proposition 2.2 and the Neumann boundary conditions, from (2.54), we obtain

$$\begin{aligned} \mathcal{E}^{n+1} - \mathcal{E}^n &\leq \Delta t \left\langle \frac{\sqrt{M^{n+1}}}{(\Delta x)^2} \tau_x \left(\frac{\rho^{n+1}}{\sqrt{M^{n+1}}} \right) + \frac{\sqrt{M^{n+1}}}{(\Delta y)^2} \tau_y \left(\frac{\rho^{n+1}}{\sqrt{M^{n+1}}} \right), \log \rho^{n+1} - c^{n+1} \right\rangle_k \\ &\quad + \left\langle \frac{\delta_x c^{n+1} - \delta_x c^n}{\Delta x}, \frac{\delta_x c^{n+1}}{\Delta x} \right\rangle_{m_x} + \left\langle \frac{\delta_y c^{n+1} - \delta_y c^n}{\Delta y}, \frac{\delta_y c^{n+1}}{\Delta y} \right\rangle_{m_y} - \left\langle c^{n+1} - c^n, \rho^n \right\rangle_k \\ &= \Delta t \left\langle \frac{\sqrt{M^{n+1}}}{(\Delta x)^2} \tau_x \left(\frac{\rho^{n+1}}{\sqrt{M^{n+1}}} \right) + \frac{\sqrt{M^{n+1}}}{(\Delta y)^2} \tau_y \left(\frac{\rho^{n+1}}{\sqrt{M^{n+1}}} \right), \log \rho^{n+1} - c^{n+1} \right\rangle_k \\ &\quad - \left\langle c^{n+1} - c^n, \delta^2 c^{n+1} + \rho^n \right\rangle_k \\ &= -\Delta t \left[\left\langle M^{n+1} \delta \left(\frac{\rho^{n+1}}{M^{n+1}} \right), \delta \left(\log \rho^{n+1} - c^{n+1} \right) \right\rangle_m + \varepsilon \left\langle \frac{c^{n+1} - c^n}{\Delta t}, \frac{c^{n+1} - c^n}{\Delta t} \right\rangle_k \right]. \end{aligned} \quad (2.55)$$

Therefore, we have completed the proof. \square

Remark 2.6. Now, we compare the discrete energy dissipation law (2.52) with the semi-analytic one (2.26). For the fully discrete five-point scheme (1.18) and (1.19), we take

$$\left(\frac{1}{\Delta x} M_{i+\frac{1}{2}, j}^{n+1} \delta_x \left(\frac{\rho}{M} \right)_{i+\frac{1}{2}, j}^{n+1}, \frac{1}{\Delta y} M_{i, j+\frac{1}{2}}^{n+1} \delta_y \left(\frac{\rho}{M} \right)_{i, j+\frac{1}{2}}^{n+1} \right) \quad (2.56)$$

as an approximation for $M^{n+1}\nabla\left(\frac{\rho^{n+1}}{M^{n+1}}\right)$ with a second-order accuracy in space. Based on the identity $M^{n+1}\nabla\left(\frac{\rho}{M}\right)^{n+1}=\rho^{n+1}\nabla(\log\rho^{n+1}-c^{n+1})$, Eq. (2.56) can be considered as

$$\left(\frac{1}{\Delta x}\rho_{i+\frac{1}{2},j}^{n+1}\delta_x(\log\rho-c)_{i+\frac{1}{2},j}^{n+1},\frac{1}{\Delta y}\rho_{i,j+\frac{1}{2}}^{n+1}\delta_y(\log\rho-c)_{i,j+\frac{1}{2}}^{n+1}\right), \quad (2.57)$$

which approximates $\rho^{n+1}\nabla(\log\rho^{n+1}-c^{n+1})$ with a second-order accuracy in space. Therefore, the discrete energy dissipation law (Theorem 2.3) gives

$$\begin{aligned} \mathcal{E}^{n+1}-\mathcal{E}^n &\leq -\Delta t\left\langle M^{n+1}\delta\left(\frac{\rho^{n+1}}{M^{n+1}}\right),\delta(\log\rho^{n+1}-c^{n+1})\right\rangle_m -\varepsilon\Delta t\left\langle\frac{c^{n+1}-c^n}{\Delta t},\frac{c^{n+1}-c^n}{\Delta t}\right\rangle_k \\ &= -\Delta t\int_{\Omega}\left[\rho^{n+1}|\nabla(\log\rho^{n+1}-c^{n+1})|^2+\varepsilon\left|\frac{c^{n+1}-c^n}{\Delta t}\right|^2\right]d\mathbf{x}+O(\Delta t(\Delta x)^2)+O(\Delta t(\Delta y)^2). \end{aligned} \quad (2.58)$$

In other words, we have shown the discrete version of the energy dissipation law for the fully discrete five-point scheme (1.18) and (1.19) matches with the semi-analytic one (2.26) with second-order accuracy in space.

Remark 2.7. It can be shown that the energy law of the ADI schemes (2.2) and (2.8) is

$$\begin{aligned} \mathcal{E}^{n+1}-\mathcal{E}^n &\leq -\Delta t\left[\left\langle\rho^{n+1}\delta(\log\rho^{n+1}-c^{n+1}),\delta(\log\rho^{n+1}-c^{n+1})\right\rangle_m +\varepsilon\left\langle\frac{c^{n+1}-c^n}{\Delta t},\frac{c^{n+1}-c^n}{\Delta t}\right\rangle_k\right] \\ &\quad -\Delta t\left\langle\mu_x\mu_y\sqrt{M^{n+1}}\tau_x\tau_y\left(\frac{\rho}{\sqrt{M}}\right)^{n+1},\log\rho^{n+1}-c^{n+1}\right\rangle_k \\ &\quad +\Delta t\left\langle c^{n+1}-c^n,\mu_x^\varepsilon\mu_y^\varepsilon\delta_x^2\delta_y^2c^{n+1}\right\rangle_k +O(\Delta t(\Delta x)^2)+O(\Delta t(\Delta y)^2). \end{aligned} \quad (2.59)$$

Notice that the high-order operators $\mu_x\mu_y\sqrt{M^{n+1}}\tau_x\tau_y\left(\frac{\rho}{\sqrt{M}}\right)^{n+1}$ and $\mu_x^\varepsilon\mu_y^\varepsilon\delta_x^2\delta_y^2c^{n+1}$ converge to zero with order $O((\Delta t)^2)$. Therefore, we know that the energy dissipation law of the ADI schemes (2.2) and (2.8) holds when the grid sizes Δx , Δy and the time step size Δt tend to zero.

2.3 A second-order scheme

Inspired by the Crank-Nicolson scheme, we can extend the previous ADI scheme to a second-order scheme in time. The preceding sections have demonstrated that our scheme exhibits second-order spatial accuracy. To achieve second-order accuracy in time, we propose an additive splitting ADI scheme that resembles a Crank-Nicolson scheme. To be specific,

$$\varepsilon\frac{c^{n+\frac{1}{2}}-c^n}{\Delta t/2}=\frac{1}{(\Delta x)^2}\delta_x^2c^{n+\frac{1}{2}}+\frac{1}{(\Delta y)^2}\delta_y^2c^n+\rho^n, \quad (2.60)$$

$$\varepsilon \frac{c^{n+1} - c^{n+\frac{1}{2}}}{\Delta t/2} = \frac{1}{(\Delta x)^2} \delta_x^2 c^{n+\frac{1}{2}} + \frac{1}{(\Delta y)^2} \delta_y^2 c^{n+1} + \rho^{n+1}, \quad (2.61)$$

and

$$\frac{\rho^{n+\frac{1}{2}} - \rho^n}{\Delta t/2} = \sqrt{M^{n+\frac{1}{2}}} \left[\frac{1}{(\Delta x)^2} \bar{\tau}_x \left(\frac{\rho^{n+\frac{1}{2}}}{\sqrt{M^{n+\frac{1}{2}}}} \right) + \frac{1}{(\Delta y)^2} \bar{\tau}_y \left(\frac{\rho^n}{\sqrt{M^{n+\frac{1}{2}}}} \right) \right], \quad (2.62)$$

$$\frac{\rho^{n+1} - \rho^{n+\frac{1}{2}}}{\Delta t/2} = \sqrt{M^{n+\frac{1}{2}}} \left[\frac{1}{(\Delta x)^2} \bar{\tau}_x \left(\frac{\rho^{n+\frac{1}{2}}}{\sqrt{M^{n+\frac{1}{2}}}} \right) + \frac{1}{(\Delta y)^2} \bar{\tau}_y \left(\frac{\rho^{n+1}}{\sqrt{M^{n+\frac{1}{2}}}} \right) \right]. \quad (2.63)$$

Adding Eq. (2.60) and Eq. (2.61), we have

$$\varepsilon \frac{c^{n+1} - c^n}{\Delta t} = \left[\frac{1}{(\Delta x)^2} \delta_x^2 c^{n+\frac{1}{2}} + \frac{1}{2(\Delta y)^2} \delta_y^2 (c^n + c^{n+1}) \right] + \frac{\rho^n + \rho^{n+1}}{2}. \quad (2.64)$$

Similarly, adding Eq. (2.62) and Eq. (2.63), we have

$$\frac{\rho^{n+1} - \rho^n}{\Delta t} = \sqrt{M^{n+\frac{1}{2}}} \left[\frac{1}{(\Delta x)^2} \bar{\tau}_x \left(\frac{\rho^{n+\frac{1}{2}}}{\sqrt{M^{n+\frac{1}{2}}}} \right) + \frac{1}{2(\Delta y)^2} \bar{\tau}_y \left(\frac{\rho^n}{\sqrt{M^{n+\frac{1}{2}}}} + \frac{\rho^{n+1}}{\sqrt{M^{n+\frac{1}{2}}}} \right) \right]. \quad (2.65)$$

Remark 2.8. The variable ρ^{n+1} is unknown in (2.61) or (2.64). To preserve the second-order time convergence, we could use $2\rho^n - \rho^{n-1}$ to approximate ρ^{n+1} . Using this approximation, it is easy to show that the truncation errors of (2.64) and (2.65) are $O(\Delta t)^2 + O((\Delta x)^2) + O((\Delta y)^2)$. Moreover, this scheme is asymptotic preserving to the quasi-static limit.

The fully-discrete equation for the first-stage of the ADI scheme Eq. (2.60) with regard to the concentration c is

$$\begin{aligned} \varepsilon c_{i,j}^{n+\frac{1}{2}} &= \frac{\mu_x}{2} \left(c_{i-1,j}^{n+\frac{1}{2}} - 2c_{i,j}^{n+\frac{1}{2}} + c_{i+1,j}^{n+\frac{1}{2}} \right) + \frac{\mu_y}{2} \left(c_{i,j-1}^n - 2c_{i,j}^n + c_{i,j+1}^n \right) + \varepsilon c_{i,j}^n + \frac{\Delta t}{2} \rho_{i,j}^n, \\ &= \frac{\mu_x}{2} \left(c_{i-1,j}^{n+\frac{1}{2}} - 2c_{i,j}^{n+\frac{1}{2}} + c_{i+1,j}^{n+\frac{1}{2}} \right) + \left[\frac{\mu_y}{2} c_{i,j-1}^n + (\varepsilon - \mu_y) c_{i,j}^n + \frac{\mu_y}{2} c_{i,j+1}^n \right] + \frac{\Delta t}{2} \rho_{i,j}^n, \end{aligned} \quad (2.66)$$

where $\mu_x = \frac{\Delta t}{(\Delta x)^2}$, $\mu_y = \frac{\Delta t}{(\Delta y)^2}$ as in Eq. (2.5). If $\varepsilon \geq \mu_y$, the second bracket on the RHS is nonnegative. Subsequently, we can prove that (2.60) preserves positivity in the same way as we did in the first-order accuracy in time ADI scheme (2.2)-(2.4). Similarly, if $\varepsilon \geq \mu_x$, then (2.61) preserves positivity. That is, our scheme (2.64) for the concentration c preserves positivity, if $\varepsilon \geq \max(\mu_x, \mu_y)$.

The fully discrete equation for the first-stage of the ADI scheme Eq. (2.62) for the density ρ is

$$\rho_{i,j}^{n+\frac{1}{2}} = \frac{\mu_x \sqrt{M_{i,j}^{n+\frac{1}{2}}}}{2} \left[\left(\frac{\rho_{i-1,j}^{n+\frac{1}{2}}}{\sqrt{M_{i-1,j}^{n+\frac{1}{2}}}} \right) + \left(\frac{\rho_{i+1,j}^{n+\frac{1}{2}}}{\sqrt{M_{i+1,j}^{n+\frac{1}{2}}}} \right) - \left(\frac{\sqrt{M_{i-1,j}^{n+\frac{1}{2}}} + \sqrt{M_{i+1,j}^{n+\frac{1}{2}}}}{M_{i,j}^{n+\frac{1}{2}}} \right) \rho_{i,j}^{n+\frac{1}{2}} \right]$$

$$+ \frac{\mu_y \sqrt{M_{i,j}^{n+\frac{1}{2}}}}{2} \left[\left(\frac{\rho_{i,j-1}^n}{\sqrt{M_{i,j-1}^{n+\frac{1}{2}}}} \right) + \left(\frac{\rho_{i,j+1}^n}{\sqrt{M_{i,j+1}^{n+\frac{1}{2}}}} \right) - \left(\frac{\sqrt{M_{i,j-1}^{n+\frac{1}{2}}} + \sqrt{M_{i,j+1}^{n+\frac{1}{2}}}}{M_{i,j}^{n+\frac{1}{2}}} \right) \rho_{i,j}^n \right] + \rho_{i,j}^n. \quad (2.67)$$

$$1 - \frac{\mu_y}{2} \left(\frac{\sqrt{M_{i,j-1}^{n+\frac{1}{2}}} + \sqrt{M_{i,j+1}^{n+\frac{1}{2}}}}{\sqrt{M_{i,j}^{n+\frac{1}{2}}}} \right) \geq 0 \quad (2.68)$$

holds for arbitrary i, j , then the first-step of the additive ADI (2.62) preserves positivity. To prove this, we reformulate (2.67) as

$$\begin{aligned} \rho_{i,j}^{n+\frac{1}{2}} = & \frac{\mu_x}{2} \left[\sqrt{M_{i-1,j}^{n+\frac{1}{2}}} M_{i,j}^{n+\frac{1}{2}} \left(\frac{\rho_{i-1,j}^{n+\frac{1}{2}}}{M_{i-1,j}^{n+\frac{1}{2}}} - \frac{\rho_{i,j}^{n+\frac{1}{2}}}{M_{i,j}^{n+\frac{1}{2}}} \right) + \sqrt{M_{i+1,j}^{n+\frac{1}{2}}} M_{i,j}^{n+\frac{1}{2}} \left(\frac{\rho_{i+1,j}^{n+\frac{1}{2}}}{M_{i+1,j}^{n+\frac{1}{2}}} - \frac{\rho_{i,j}^{n+\frac{1}{2}}}{M_{i,j}^{n+\frac{1}{2}}} \right) \right] \\ & + \left[1 - \frac{\mu_y}{2} \left(\frac{\sqrt{M_{i,j-1}^{n+\frac{1}{2}}} + \sqrt{M_{i,j+1}^{n+\frac{1}{2}}}}{\sqrt{M_{i,j}^{n+\frac{1}{2}}}} \right) \right] \rho_{i,j}^n + \frac{\mu_y \sqrt{M_{i,j}^{n+\frac{1}{2}}}}{2\sqrt{M_{i,j-1}^{n+\frac{1}{2}}}} \rho_{i,j-1}^n + \frac{\mu_y \sqrt{M_{i,j}^{n+\frac{1}{2}}}}{2\sqrt{M_{i,j+1}^{n+\frac{1}{2}}}} \rho_{i,j+1}^n. \end{aligned} \quad (2.69)$$

We assume that $\rho_{i,j}^n$ is nonnegative and the condition (2.68) holds for all i, j , then the last three terms in Eq. (2.69) are nonnegative. Using the same argument in the proof of Theorem 2.1 again, let (k, l) be the indices satisfy $\rho_{k,l}^{n+\frac{1}{2}} / M_{k,l}^{n+\frac{1}{2}} = \min_{i,j} \{ \rho_{i,j}^{n+\frac{1}{2}} / M_{i,j}^{n+\frac{1}{2}} \}$. The terms in the first bracket of the RHS of Eq. (2.69) are nonnegative for $(i, j) = (k, l)$. From Eq. (2.69) and $M_{k,l}^{n+\frac{1}{2}} \geq 0$, we have $\rho_{k,l}^{n+\frac{1}{2}} \geq 0$, then $\rho_{k,l}^{n+\frac{1}{2}} / M_{k,l}^{n+\frac{1}{2}} \geq 0$. That is, $\rho_{i,j}^{n+\frac{1}{2}} / M_{i,j}^{n+\frac{1}{2}} \geq 0$ for all i, j because $\rho_{k,l}^{n+\frac{1}{2}} / M_{k,l}^{n+\frac{1}{2}} \geq 0$ is the minimum value from the definition. Similarly, if

$$1 - \frac{\mu_x}{2} \left(\frac{\sqrt{M_{i-1,j}^{n+\frac{1}{2}}} + \sqrt{M_{i+1,j}^{n+\frac{1}{2}}}}{\sqrt{M_{i,j}^{n+\frac{1}{2}}}} \right) \geq 0 \quad (2.70)$$

holds for arbitrary i, j , then the second-step of the additive ADI (2.63) preserves positivity. That is, the scheme (2.65) preserves positivity under these two inequality conditions (2.68) and (2.70).

Remark 2.9. We have proved this additive ADI scheme preserving positivity and it is straight forward to verify the mass conservation similar to the previous section. How-

ever, we cannot verify the energy dissipation law for the fully discrete scheme (2.64) and (2.65) since it is hard to deal with $\rho_{i,j}^n / \sqrt{M_{i,j}^{n+\frac{1}{2}}}$ and $\rho_{i,j}^{n+1} / \sqrt{M_{i,j}^{n+\frac{1}{2}}}$.

3 Numerical experiments

The solution to Keller-Segel equations have several important properties, such as positivity preservation, mass preservation, asymptotic behavior. Furthermore, the solution blows up when the initial mass is great than some critical value. In the following, we verify the order of convergence for two ADI schemes first. Then, we compare the computational time of our ADI schemes (2.2) and (2.8) with the standard five-point method (2.1) and (2.5). As we will see in the following results, the ADI scheme significantly reduces the computational cost.

3.1 The order of convergence

In this subsection, we focus on checking the order of accuracy of the ADI schemes (2.3)-(2.4) and (2.6)-(2.7). In order to verify the order of convergence, we construct an exact solution of the 2D Keller-Segel equations (1.1) and (1.2) with added known terms. We start with the following exact solutions

$$\rho(x,y,t) = 4e^{-(t+x^2+y^2)}, \quad c(x,y,t) = e^{-(t+\frac{x^2+y^2}{2})}, \quad (3.1)$$

in the square domain $\Omega = (-1,1) \times (-1,1)$.

Denoting

$$F_1(x,y,t) = [c(x,y,t)(3x^2+3y^2-2) - 4(x^2+y^2) + 3]\rho(x,y,t), \quad (3.2)$$

$$F_2(x,y,t) = (2-\varepsilon-x^2-y^2)c(x,y,t) - \rho(x,y,t), \quad (3.3)$$

the solution in Eq. (3.1) satisfies the following modified Keller-Segel system

$$\partial_t \rho = \Delta \rho - \nabla \cdot (\rho \nabla c) + F_1, \quad \varepsilon \partial_t c = \Delta c + \rho + F_2, \quad (3.4)$$

where we choose $\varepsilon = 1$ in this subsection.

To investigate the spatial convergence order, we fix time step $\Delta t = 10^{-6}$ but vary the spatial grid sizes $\Delta x = \Delta y = 0.1, 0.05, 0.025, 0.0125$. We examine the error in maximum norm at the output time $T = 10^{-5}$.

$$\text{error}_{\Delta x} = \|f_{\Delta x}(T) - f_{exact}(T)\|_{\infty} := \max_{i,j} |f_{\Delta x}(x_i, y_j, T) - f_{exact}(x_i, y_j, T)|, \quad (3.5)$$

where $f_{\Delta x}$ and f_{exact} denote the numerical solution with mesh size Δx and the exact solution respectively.

Table 1: The spatial convergence order of the ADI scheme Eqs. (2.3)-(2.4) and (2.6)-(2.7): Errors of density ρ and c for different mesh sizes.

$\Delta x = \Delta y$	Maximum error in ρ	Order	Maximum error in c	Order
0.1	2.1261E-07	–	4.9951E-08	–
0.05	5.3292E-08	1.9962	1.2530E-08	1.9951
0.025	1.3335E-08	1.9987	3.1596E-09	1.9876
0.0125	3.3376E-09	1.9983	8.1621E-10	1.9527

Table 2: The time convergence order of the ADI scheme Eqs. (2.3)-(2.4) and (2.6)-(2.7): Errors of density ρ and c for different time step sizes.

Δt	Maximum error in ρ	Order	Maximum error in c	Order
0.05	0.0093	–	0.0133	–
0.025	0.0043	1.1129	0.0070	0.9260
0.0125	0.0021	1.0339	0.0036	0.9593
0.00625	9.9789E-04	1.0734	0.0018	1.0000

To investigate the time convergence order, we fix the grid size in space $\Delta x = \Delta y = 0.001$ and compare the errors with different time steps $\Delta t = 0.05, 0.025, 0.0125, 0.00625$, and the output time is $T = 0.1$.

$$\text{error}_{\Delta t} = \|f_{\Delta t}(T) - f_{exact}(T)\|_{\infty} := \max_{i,j} |f_{\Delta t}(x_i, y_j, T) - f_{exact}(x_i, y_j, T)|, \quad (3.6)$$

where $f_{\Delta t}$ denotes the numerical solution with time step Δt .

The errors with different mesh sizes and the numerical order of convergence are presented in Table 1. The numerical order is calculated as $\log_2(\text{error}_{2\Delta x}/\text{error}_{\Delta x})$ and the results show second-order accuracy in space. Table 2 shows the errors with different time step sizes and the numerical order of convergence in time. Similarly, the numerical order is calculated as $\log_2(\text{error}_{2\Delta t}/\text{error}_{\Delta t})$ and the results confirm the first-order accuracy in time.

3.2 Second-order convergence in time

In this subsection, we follow the same example presented in Sec. 3.1 to verify the order of accuracy of the additive ADI scheme (2.60)-(2.61) and (2.62)-(2.63).

Our goal is to verify the additive ADI scheme for the following equations:

$$\partial_t \rho = \Delta \rho - \nabla \cdot (\rho \nabla c) + F_1 = \nabla \cdot \left(M \nabla \left(\frac{\rho}{M} \right) \right) + F_1, \quad (3.7)$$

$$\varepsilon \partial_t c = \Delta c + \rho + F_2, \quad (3.8)$$

where $M = e^c$. The semi-discrete scheme is

$$\varepsilon \frac{c^{n+\frac{1}{2}} - c^n}{\Delta t/2} = \frac{1}{(\Delta x)^2} \delta_x^2 c^{n+\frac{1}{2}} + \frac{1}{(\Delta y)^2} \delta_y^2 c^n + \rho^n + F_2^n, \quad (3.9)$$

$$\varepsilon \frac{c^{n+1} - c^{n+\frac{1}{2}}}{\Delta t/2} = \frac{1}{(\Delta x)^2} \delta_x^2 c^{n+\frac{1}{2}} + \frac{1}{(\Delta y)^2} \delta_y^2 c^{n+1} + \rho^{n+1} + F_2^{n+1}, \quad (3.10)$$

and

$$\frac{\rho^{n+\frac{1}{2}} - \rho^n}{\Delta t/2} = \sqrt{M^{n+\frac{1}{2}}} \left[\frac{1}{(\Delta x)^2} \bar{\tau}_x \left(\frac{\rho^{n+\frac{1}{2}}}{\sqrt{M^{n+\frac{1}{2}}}} \right) + \frac{1}{(\Delta y)^2} \bar{\tau}_y \left(\frac{\rho^n}{\sqrt{M^{n+\frac{1}{2}}}} \right) \right] + F_1^n, \quad (3.11)$$

$$\frac{\rho^{n+1} - \rho^{n+\frac{1}{2}}}{\Delta t/2} = \sqrt{M^{n+\frac{1}{2}}} \left[\frac{1}{(\Delta x)^2} \bar{\tau}_x \left(\frac{\rho^{n+\frac{1}{2}}}{\sqrt{M^{n+\frac{1}{2}}}} \right) + \frac{1}{(\Delta y)^2} \bar{\tau}_y \left(\frac{\rho^{n+1}}{\sqrt{M^{n+\frac{1}{2}}}} \right) \right] + F_1^{n+1}. \quad (3.12)$$

The semi-discrete scheme is equivalent to

$$\begin{aligned} \varepsilon c^{n+\frac{1}{2}} - \frac{\mu_x}{2} \delta_x^2 c^{n+\frac{1}{2}} &= \varepsilon c^n + \frac{\mu_y}{2} \delta_y^2 c^n + \frac{\Delta t}{2} (\rho^n + F_2^n), \\ \varepsilon c^{n+1} - \frac{\mu_y}{2} \delta_y^2 c^{n+1} &= \varepsilon c^{n+\frac{1}{2}} + \frac{\mu_x}{2} \delta_x^2 c^{n+\frac{1}{2}} + \frac{\Delta t}{2} (\rho^{n+1} + F_2^{n+1}), \end{aligned} \quad (3.13)$$

and

$$\begin{aligned} \rho^{n+\frac{1}{2}} - \frac{\mu_x}{2} \sqrt{M^{n+\frac{1}{2}}} \bar{\tau}_x \left(\frac{\rho^{n+\frac{1}{2}}}{\sqrt{M^{n+\frac{1}{2}}}} \right) &= \rho^n + \frac{\mu_y}{2} \sqrt{M^{n+\frac{1}{2}}} \bar{\tau}_y \left(\frac{\rho^n}{\sqrt{M^{n+\frac{1}{2}}}} \right) + \frac{\Delta t}{2} F_1^n, \\ \rho^{n+1} - \frac{\mu_y}{2} \sqrt{M^{n+\frac{1}{2}}} \bar{\tau}_y \left(\frac{\rho^{n+1}}{\sqrt{M^{n+\frac{1}{2}}}} \right) &= \rho^{n+\frac{1}{2}} + \frac{\mu_x}{2} \sqrt{M^{n+\frac{1}{2}}} \bar{\tau}_x \left(\frac{\rho^{n+\frac{1}{2}}}{\sqrt{M^{n+\frac{1}{2}}}} \right) + \frac{\Delta t}{2} F_1^{n+1}. \end{aligned} \quad (3.14)$$

To investigate the time convergence order, we fix the grid size in space $\Delta x = \Delta y = 0.001$ and compare the errors with different time steps $\Delta t = 0.01, 0.005, 0.0025, 0.00125$, and the output time is $T = 0.04$. We choose the parameter $\varepsilon = 1$ in this case. Table 3 shows the errors with different time step sizes, which confirms the second-order accuracy in time.

Stability. To numerically investigate the stability of the 2nd-order ADI scheme (2.60)-(2.63), we compute the solution to the modified Keller-Segel system (3.4), the same example as in Section 3.1. We summarize the relative L^2 errors of the density ρ at final time $T = 5$ computed by the 2nd-order ADI scheme (2.60)-(2.63) with various mesh sizes and time step sizes in Table 4. The numerical results show that the errors mainly come from the time integration for the range of grid sizes and time step sizes. The results are stable for the time step size Δt as large as 0.2 and the grid sizes Δx and Δy as small as 0.002, suggesting that the 2nd-order ADI scheme is stable. We obtain similar results for the concentration c . The extrapolation $2\rho^n - \rho^{n-1}$ used in the 2nd-order ADI scheme does not affect the stability. In addition, the first-order semi-discrete scheme (1.4) and (1.5) is shown to be stable for small initial data and $\Delta t \|\nabla \rho^n\| < 1$ in [25]. The numerical stability is verified for the 1st-order ADI scheme (2.2) and (2.8) from similar tests as above.

Table 3: The time convergence order of the additive ADI scheme Eqs. (2.60)-(2.61) and (2.62)-(2.63): Errors of density ρ and c for different time step sizes.

Δt	Maximum error in ρ	Order	Maximum error in c	Order
0.01	4.7003E-05	–	1.2824E-05	–
0.005	1.1076E-05	2.0853	3.1129E-06	2.0425
0.0025	2.5185E-06	2.1368	7.2538E-07	2.1014
0.00125	6.6010E-07	1.9318	1.5921E-07	2.1878

Table 4: The relative L^2 errors of the density ρ at final time $T = 5$ with various mesh sizes and time step sizes for the 2nd-order ADI scheme (2.60)-(2.63).

Δt	$\Delta x = \Delta y = 0.05$	$\Delta x = \Delta y = 0.02$	$\Delta x = \Delta y = 0.01$	$\Delta x = \Delta y = 0.002$
0.2	0.0080	0.0084	0.0085	0.0086
0.1	0.0017	0.0020	0.0021	0.0021
0.05	4.7422E-04	4.6599E-04	5.0646E-04	5.2215E-04
0.01	5.6766E-04	8.1606E-05	1.9401E-05	2.0315E-05

3.3 Efficiency

Blow-up is one of the most important properties of Keller-Segel system [2, 14]. The solutions of Keller-Segel equations blow up in finite time if the initial mass is large than a critical value. In order to investigate the solutions close to the blow-up time, extremely fine grid is needed. Developing a highly efficient numerical scheme becomes important to reduce computational cost. The original five-point method need to solve (2.1) and (2.5) require solving four sparse $N_x N_y \times N_x N_y$ linear systems using an iterative method such as conjugate gradient method. It still results in relatively high computational cost, especially in the case of higher dimensions. It is well known that ADI schemes are a type of fast direct method to solve 2D or higher dimensional parabolic partial differential equations. For the first-step of the ADI scheme for the density (2.6), we only need to solve N_y decoupled tridiagonal linear systems of size $N_x \times N_x$. The computational complexity is similar for the rest substeps of the ADI scheme Eqs. (2.7), (2.3) and (2.4). In this subsection, we compare the computational efficiency of our ADI scheme with that of the five-point scheme. Here we use the conjugate gradient method to solve the linear system for the original five-point scheme.

To compare the computational costs, we use the example in Subsection 3.1 with known exact solutions. We take domain $\Omega = [-5, 5] \times [-5, 5]$, time step $\Delta t = 0.001$, and the final time is $T = 1$, and different space grid sizes $N_x = N_y = 80, 160, 320, 640$ respectively. The running times of our ADI scheme (2.3)-(2.4) and (2.6)-(2.7) and the original method (2.1), (2.5) are presented in Table 5. The execution times are measured using MATLAB scripts on a personal computer with Intel(R) Core(TM) i5-8265U CPU @ 1.60GHz 1.80GHz and

Table 5: Comparison between the running times in (seconds) of the ADI scheme (2.3)-(2.4) and (2.6)-(2.7) and those of the original five-point scheme (2.1) and (2.5) (ORIG for short) with different mesh sizes. N denotes the total number of unknowns in the system.

N	ADI	ORIG
$2 \cdot 80^2$	3.34s	20.34s
$2 \cdot 160^2$	10.55s	73.60s
$2 \cdot 320^2$	38.05s	296.76s
$2 \cdot 640^2$	145.69s	1530.91s

8 GB RAM. The ADI scheme reduces the computational cost dramatically, as we expect. Both running times increase linearly with the number of unknowns, $N = 2N_x N_y$ until the original scheme runs into the limitation of the PC memory. The ADI scheme is about seven times faster than that of the original one. It is worth pointing out the linear systems corresponding to the ADI scheme are solved directly and the solutions to the linear systems are accurate up to round-off errors, while the tolerance of the CG iterative solver is set to be 10^{-10} thus the numerical results from the original scheme are less accurate. Therefore, the ADI scheme could be used to capture more accurate asymptotic behavior near the blow-up of the solutions.

3.4 An illustrative example

To demonstrate the conserved properties of the numerical schemes, such as the mass conservation and the energy dissipation law, in this subsection we present the evolution of the relevant quantities by solving the 2D Keller-Segel equations (1.1) and (1.2) with periodic or Neumann-type boundary conditions.

Consider the original Keller-Segel equations (1.1) and (1.2) with the following initial conditions:

$$\rho(x, y, 0) = 50e^{-60(x^2+y^2)}, \quad c(x, y, 0) = 50e^{-30(x^2+y^2)}. \quad (3.15)$$

The nonnegative constant is chosen as $\varepsilon = 1$ and the spatial domain $\Omega = (-1, 1) \times (-1, 1)$. We set the mesh sizes $\Delta x = \Delta y = 0.02$ and the time step size $\Delta t = 0.0001$. In order to verify the proposed ADI scheme (2.2), (2.8) is positivity-preserving, we plot the evolution of the quantities $\min_{i,j} \{\rho_{i,j}\}$ and $\min_{i,j} \{c_{i,j}\}$ in Figure 1. The quantities that lead to the conservation of mass defined in (2.14), (2.15) together with the total mass $\rho_{\text{tot}}(t) := \int_{\Omega} \rho dx dy$ and $c_{\text{tot}}(t) = \int_{\Omega} c dx dy$ for periodic or the vanishing Neumann boundary conditions are also shown in Figure 2 and Figure 3, respectively. The numerical results show that the mass is conserved up to the round-off level up to the time $t = 2$. Note that the total mass of c , $c_{\text{tot}}(t)$ increases linearly in time according to $c_{\text{tot}}(t) = c_{\text{tot}}(0) + \rho_{\text{tot}}(0)t$. In Figure 4, we show the evolution of the discrete free energy \mathcal{E}^n defined by (2.51) for this case with periodic boundary condition and compare the energy decay rate $(\mathcal{E}^{n+1} - \mathcal{E}^n) / \Delta t$ and the RHS

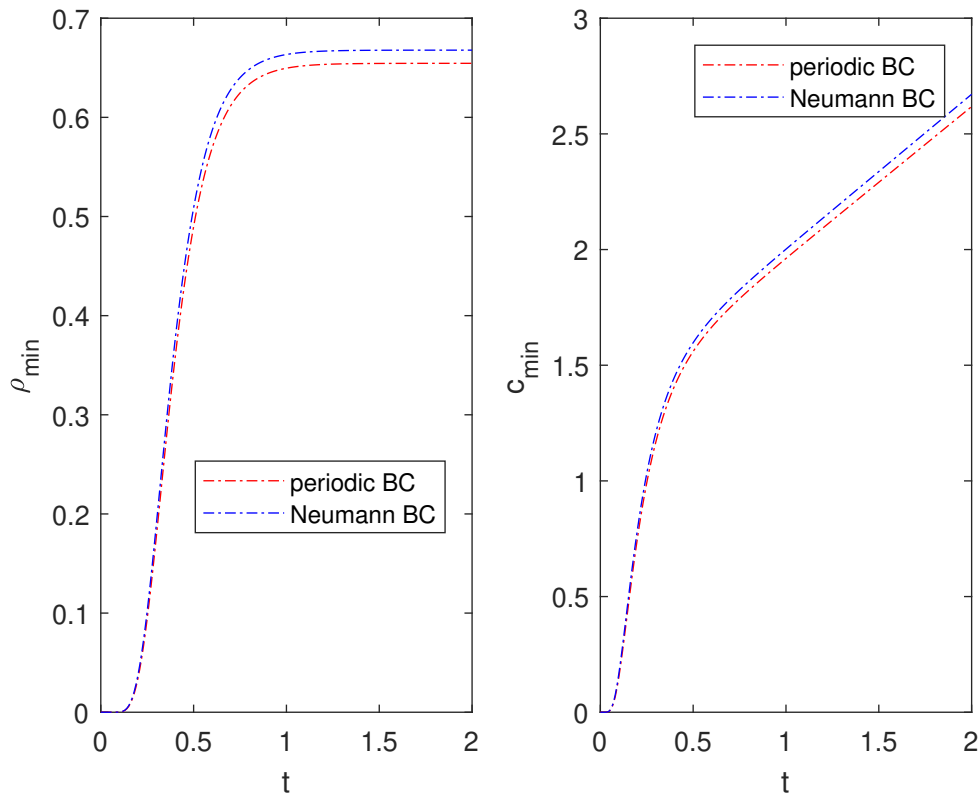


Figure 1: The evolution of the minimum values of the density ρ and the concentration c for the solution of the Keller-Segel equations (1.1) and (1.2) with $\epsilon = 1$, the initial condition (3.15) and the periodic or vanishing Neumann boundary conditions. (Left) $\rho_{\min} := \min_{i,j} \{\rho_{i,j}\}$. (Right) $c_{\min} := \min_{i,j} \{c_{i,j}\}$.

of (2.52) divided by Δt . The numerical results show that the inequality (2.52) holds all the time. The numerical results for vanishing Neumann boundary conditions are similar as shown in Figure 5.

4 Conclusion

We have presented two efficient finite difference schemes for solving the 2D Keller-Segel equations based on ADI method. Both schemes achieve second-order accuracy in space. One of the schemes exhibits first-order accuracy in time while unconditionally preserving positivity and the energy dissipation law asymptotically. The other scheme achieves second-order accuracy in time, but it only preserves positivity under certain conditions.

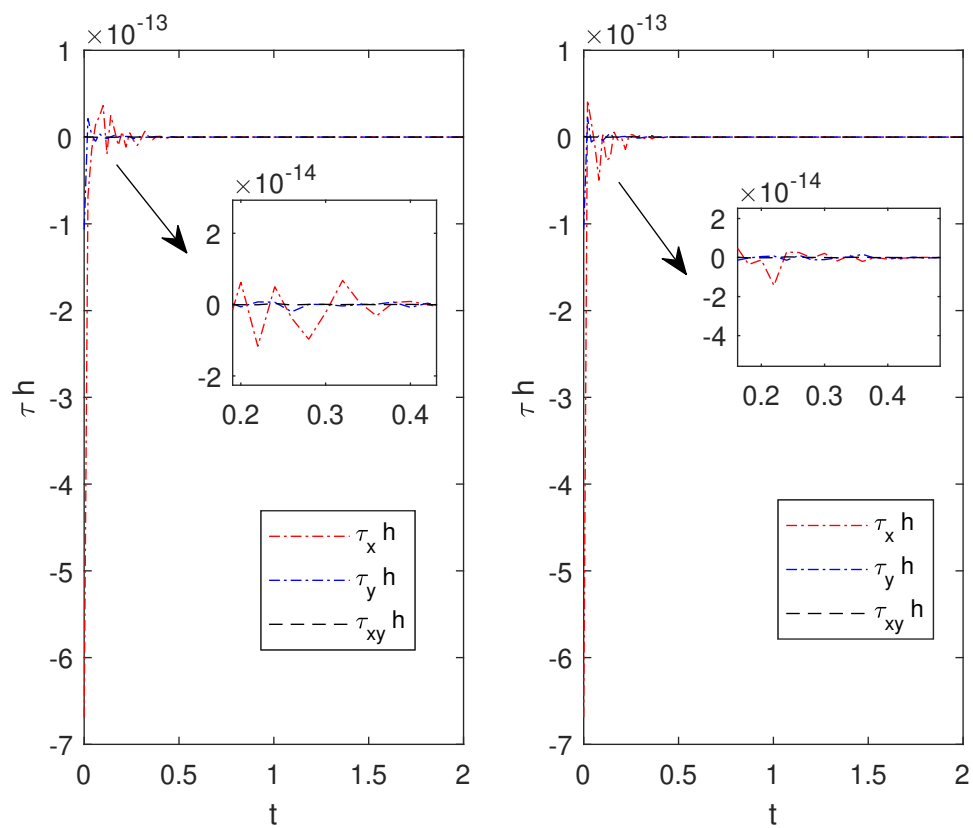


Figure 2: The quantities defined in (2.14) and (2.15) for the solution of the Keller-Segel equations (1.1) and (1.2) with $\epsilon=1$ and the initial condition (3.15). (Left) Periodic boundary conditions. (Right) Vanishing Neumann boundary conditions.

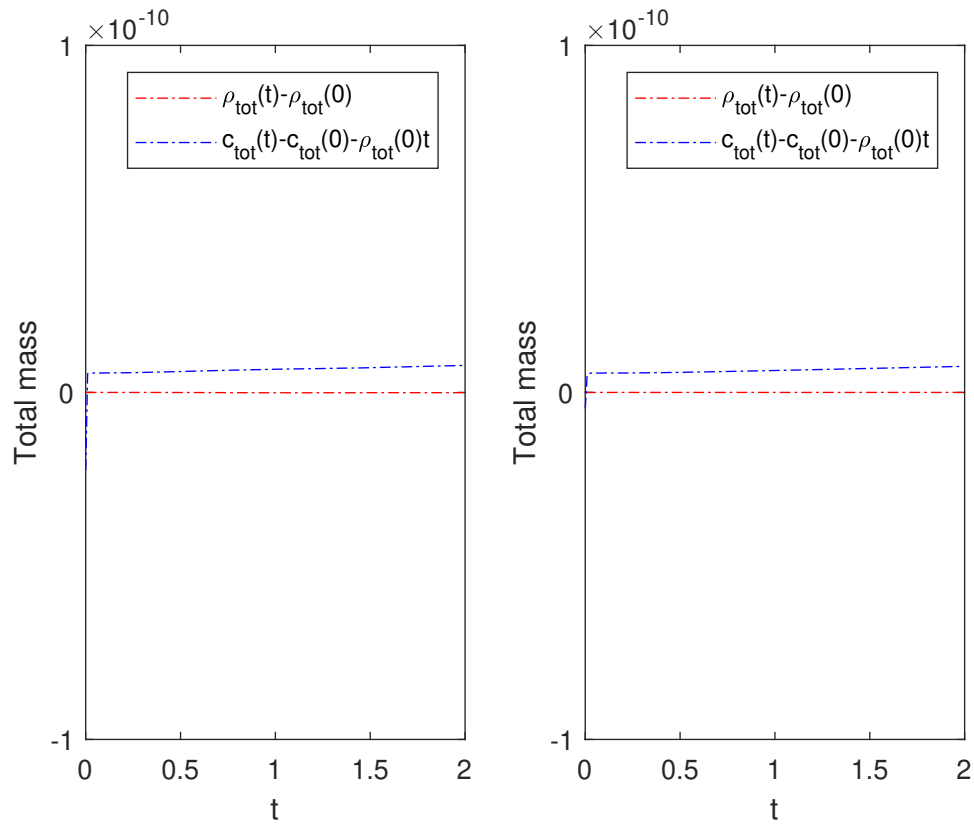


Figure 3: The evolution of the total mass compared with the initial values, namely $\rho_{\text{tot}}(t) - \rho_{\text{tot}}(0)$ and $c_{\text{tot}}(t) - c_{\text{tot}}(0) - \rho_{\text{tot}}(0)t$, for the solution of the Keller-Segel equations (1.1) and (1.2) with $\epsilon = 1$ and the initial condition (3.15). (Left) Periodic boundary conditions. (Right) Vanishing Neumann boundary conditions.

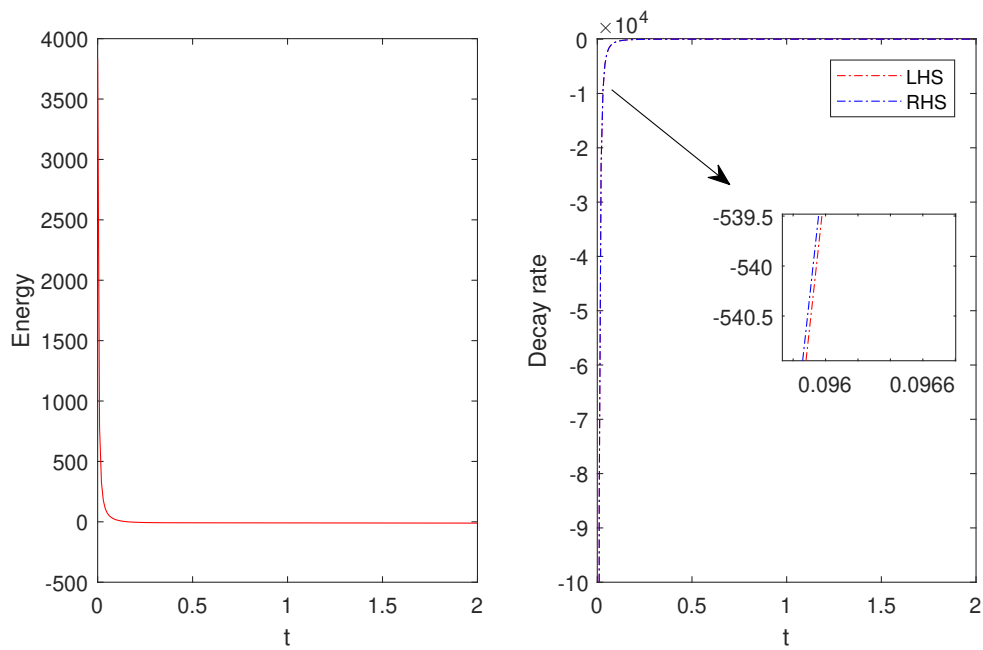


Figure 4: (Left) The evolution of the discrete free energy \mathcal{E}^n (2.51) for the solution of the Keller-Segel equations (1.1) and (1.2) with $\epsilon = 1$ and the initial condition (3.15) with periodic boundary conditions. (Right) The corresponding the energy decay rate $(\mathcal{E}^{n+1} - \mathcal{E}^n)/\Delta t$ and the RHS of (2.52) divided by Δt .

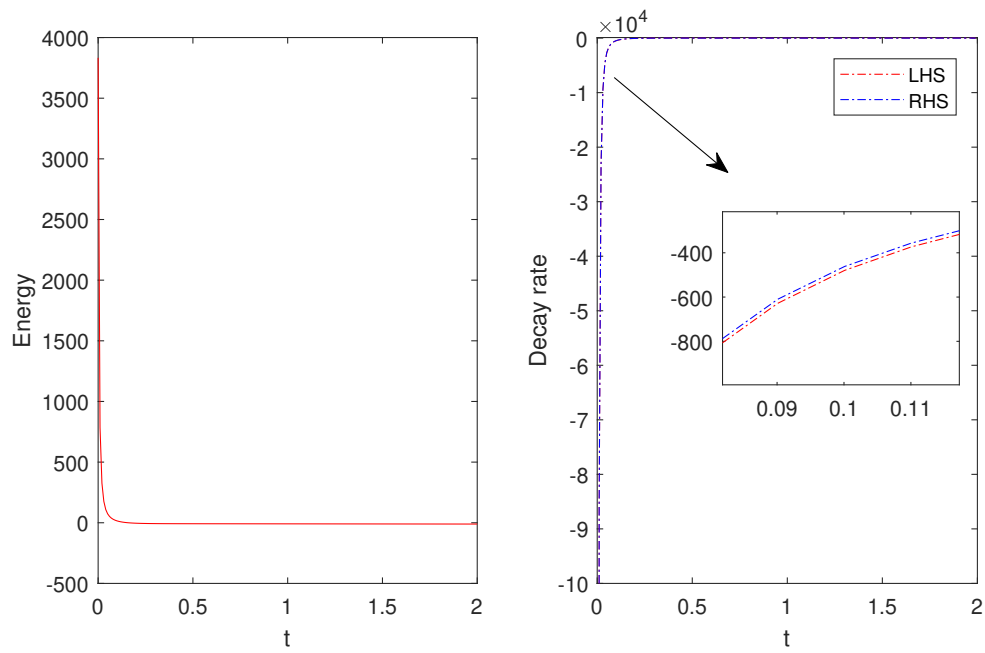


Figure 5: (Left) The evolution of the discrete free energy \mathcal{E}^n (2.51) for the solution of the Keller-Segel equations (1.1) and (1.2) with $\epsilon = 1$ and the initial condition (3.15) with vanishing Neumann boundary conditions. (Right) The corresponding the energy decay rate $(\mathcal{E}^{n+1} - \mathcal{E}^n) / \Delta t$ and the RHS of (2.52) divided by Δt .

Furthermore, we demonstrate that our schemes outperform the standard five-point scheme in terms of computational cost.

There are still important aspects that require further investigation. First, although the additive ADI scheme attains second-order accuracy in time, its ability to preserve positivity is conditional. This limitation hinders its widespread adoption. Second, the energy dissipation law for the first-order ADI scheme holds asymptotically rather than exactly. Third, we can deduce the Keller-Segel equations from the respective free energy using the energetic variational approach. This approach offers an alternative method for investigating the blow-up solutions of the Keller-Segel equations, known as the Lagrangian scheme. Additionally, we employ the semi-implicit scheme to decouple the two nonlinear partial equations. However, it is important to note that the explicit components of the semi-implicit scheme may introduce instability issues when dealing with large initial mass conditions. Further investigation is warranted in this regard.

Acknowledgments

This work is partially supported by DOE DE-SC0022276. C Liu's research is partially supported by NSF grants DMS-1950868, DMS-2153029 and DMS-2118181. Lu would like to thank Yiwei Wang for helpful discussions.

References

- [1] L. Almeida, F. Bubba, B. Perthame, and C. Pouchol. Energy and implicit discretization of the fokker-planck and keller-segel type equations. *Networks and Heterogeneous Media*, 14(1):23–41, 2019.
- [2] N. Bellomo, A. Bellouquid, Y. Tao, and M. Winkler. Toward a mathematical theory of Keller–Segel models of pattern formation in biological tissues. *Mathematical Models and Methods in Applied Sciences*, 25(09):1663–1763, 2015.
- [3] M. Bessemoulin-Chatard and A. Jüngel. A finite volume scheme for a Keller–Segel model with additional cross-diffusion. *IMA Journal of Numerical Analysis*, 34(1):96–122, 2013.
- [4] V. Calvez and L. Corrias. The parabolic-parabolic Keller-Segel model in \mathbb{R}^2 . *Communications in Mathematical Sciences*, 6(2):417 – 447, 2008.
- [5] J. A. Carrillo, A. Chertock, and Y. Huang. A finite-volume method for nonlinear nonlocal equations with a gradient flow structure. *Communications in Computational Physics*, 17(1):233–258, 2015.

- [6] A. Chertock and A. Kurganov. A second-order positivity preserving central-upwind scheme for chemotaxis and haptotaxis models. *Numerische Mathematik*, 111:169–205, 2008.
- [7] C. M. Elliott and A. M. Stuart. The global dynamics of discrete semilinear parabolic equations. *SIAM Journal on Numerical Analysis*, 30(6):1622–1663, 1993.
- [8] Y. Epshteyn. Upwind-difference potentials method for Patlak-Keller-Segel chemotaxis model. *Journal of Scientific Computing*, 53:689–713, 2012.
- [9] Y. Epshteyn and A. Izmirliglu. Fully discrete analysis of a discontinuous finite element method for the Keller-Segel chemotaxis model. *Journal of Scientific Computing*, 40:211–256, 2009.
- [10] Y. Epshteyn and A. Kurganov. New interior penalty discontinuous Galerkin methods for the Keller–Segel chemotaxis model. *SIAM Journal on Numerical Analysis*, 47(1):386–408, 2009.
- [11] A. Flavell, J. Kabre, and X. Li. An energy-preserving discretization for the Poisson–Nernst–Planck equations. *Journal of Computational Electronics*, 16(2):431–441, June 2017.
- [12] J. Forster. *Mathematical modeling of complex fluids*. PhD thesis, Universität Würzburg, 2013.
- [13] M.-H. Giga, A. Kirshtein, and C. Liu. Variational modeling and complex fluids. *Handbook of mathematical analysis in mechanics of viscous fluids*, pages 1–41, 2017.
- [14] T. Hillen and K. J. Painter. A user’s guide to pde models for chemotaxis. *Journal of Mathematical Biology*, 58:183–217, 2009.
- [15] D. Horstmann. From 1970 until present : the Keller-Segel model in chemotaxis and its consequences I. *Jahresbericht der Deutschen Mathematiker-Vereinigung*, 105(3):103–165, 2003.
- [16] F. Huang and J. Shen. Bound/positivity preserving and energy stable scalar auxiliary variable schemes for dissipative systems: Applications to Keller-Segel and Poisson-Nernst-Planck equations. *SIAM Journal on Scientific Computing*, 43(3):A1832–A1857, 2021.
- [17] E. F. Keller and L. A. Segel. Initiation of slime mold aggregation viewed as an instability. *Journal of Theoretical Biology*, 26(3):399–415, 1970.
- [18] E. F. Keller and L. A. Segel. Traveling bands of chemotactic bacteria: A theoretical analysis. *Journal of Theoretical Biology*, 30(2):235–248, 1971.

- [19] A. Kurganov and M. Lukáčová-Medvidová. Numerical study of two-species chemotaxis models. *Discrete and Continuous Dynamical Systems - B*, 19(1):131–152, 2014.
- [20] X. H. Li, C.-W. Shu, and Y. Yang. Local discontinuous Galerkin method for the Keller-Segel chemotaxis model. *Journal of Scientific Computing*, 73:943–967, 2017.
- [21] C. Liu, C. Wang, S. M. Wise, X. Yue, and S. Zhou. A second order accurate, positivity preserving numerical method for the Poisson-Nernst-Planck system and its convergence analysis. *Journal of Scientific Computing*, 97(1):23, Sep 2023.
- [22] C. Liu and Y. Wang. A variational Lagrangian scheme for a phase-field model: A discrete energetic variational approach. *SIAM Journal on Scientific Computing*, 42(6):B1541–B1569, 2020.
- [23] H. Liu and W. Maimaitiyiming. Efficient, positive, and energy stable schemes for multi-D Poisson-Nernst-Planck systems. *Journal of Scientific Computing*, 87(3):92, May 2021.
- [24] H. Liu and W. Maimaitiyiming. A dynamic mass transport method for Poisson-Nernst-Planck equations. *Journal of Computational Physics*, 473:111699, 2023.
- [25] J.-G. Liu, L. Wang, and Z. Zhou. Positivity-preserving and asymptotic preserving method for 2d Keller-Segel equations. *Mathematics of Computation*, 87(311):1165–1189, 2018.
- [26] C. S. Patlak. Random walk with persistence and external bias. *The bulletin of mathematical biophysics*, 15:311–338, 1953.
- [27] B. Perthame. *Transport Equations in Biology*. Frontiers in Mathematics. Birkhäuser Basel, 2006.
- [28] J. Shen and J. Xu. Unconditionally bound preserving and energy dissipative schemes for a class of Keller–Segel equations. *SIAM Journal on Numerical Analysis*, 58(3):1674–1695, 2020.
- [29] J. Shen and J. Xu. Unconditionally positivity preserving and energy dissipative schemes for Poisson-Nernst-Planck equations. *Numerische Mathematik*, 148(3):671–697, Jul 2021.
- [30] J. Shen, J. Xu, and J. Yang. A new class of efficient and robust energy stable schemes for gradient flows. *SIAM Review*, 61(3):474–506, 2019.
- [31] J. Shen and X. Yang. Numerical approximations of Allen-Cahn and Cahn-Hilliard equations. *Discrete and Continuous Dynamical Systems*, 28(4):1669–1691, 2010.

- [32] X. Yang. Linear, first and second-order, unconditionally energy stable numerical schemes for the phase field model of homopolymer blends. *Journal of Computational Physics*, 327:294–316, 2016.
- [33] J. Zhao, Q. Wang, and X. Yang. Numerical approximations for a phase field dendritic crystal growth model based on the invariant energy quadratization approach. *International Journal for Numerical Methods in Engineering*, 110(3):279–300, 2017.
- [34] G. Zhou and N. Saito. Finite volume methods for a Keller–Segel system: discrete energy, error estimates and numerical blow-up analysis. *Numerische Mathematik*, 135:265–311, 2017.
- [35] J. Zhu, L.-Q. Chen, J. Shen, and V. Tikare. Coarsening kinetics from a variable-mobility Cahn-Hilliard equation: Application of a semi-implicit fourier spectral method. *Phys. Rev. E*, 60:3564–3572, Oct 1999.

A Detailed Expressions for the Operators τ_x, τ_y and $\tau_x \tau_y$

In order to derive the truncation errors and prove the positivity preservation and mass conservation, we expand the operators τ_x, τ_y and $\tau_x \tau_y$ fully

$$\begin{aligned} \tau_x h_{i,j}^{n+1} &:= \frac{1}{\sqrt{M_{i,j}^{n+1}}} \delta_x \left(M_{i,j}^{n+1} \delta_x \left(\frac{h^{n+1}}{\sqrt{M^{n+1}}} \right)_{i,j} \right) \\ &= \frac{1}{\sqrt{M_{i,j}^{n+1}}} \left[\sqrt{M_{i,j}^{n+1} M_{i+1,j}^{n+1}} \left(\frac{h_{i+1,j}^{n+1}}{\sqrt{M_{i+1,j}^{n+1}}} - \frac{h_{i,j}^{n+1}}{\sqrt{M_{i,j}^{n+1}}} \right) - \sqrt{M_{i-1,j}^{n+1} M_{i,j}^{n+1}} \left(\frac{h_{i,j}^{n+1}}{\sqrt{M_{i,j}^{n+1}}} - \frac{h_{i-1,j}^{n+1}}{\sqrt{M_{i-1,j}^{n+1}}} \right) \right]. \end{aligned} \quad (\text{A.1})$$

Similarly, we have

$$\begin{aligned} \tau_y h_{i,j}^{n+1} &:= \frac{1}{\sqrt{M_{i,j}^{n+1}}} \delta_y \left(M_{i,j}^{n+1} \delta_y \left(\frac{h_{i,j}^{n+1}}{\sqrt{M_{i,j}^{n+1}}} \right) \right) \\ &= \frac{1}{\sqrt{M_{i,j}^{n+1}}} \left[\sqrt{M_{i,j}^{n+1} M_{i,j+1}^{n+1}} \left(\frac{h_{i,j+1}^{n+1}}{\sqrt{M_{i,j+1}^{n+1}}} - \frac{h_{i,j}^{n+1}}{\sqrt{M_{i,j}^{n+1}}} \right) - \sqrt{M_{i,j-1}^{n+1} M_{i,j}^{n+1}} \left(\frac{h_{i,j}^{n+1}}{\sqrt{M_{i,j}^{n+1}}} - \frac{h_{i,j-1}^{n+1}}{\sqrt{M_{i,j-1}^{n+1}}} \right) \right]. \end{aligned} \quad (\text{A.2})$$

For the composite operator $\tau_x \tau_y$, we have

$$\begin{aligned} \tau_x \tau_y h_{i,j}^{n+1} &= \frac{1}{\sqrt{M_{i,j}^{n+1}}} \delta_x \left[M_{i,j}^{n+1} \delta_x \left(\frac{\tau_y h}{\sqrt{M}} \right)_{i,j}^{n+1} \right] \\ &= \frac{M_{i+\frac{1}{2},j}^{n+1}}{\sqrt{M_{i,j}^{n+1}}} \left[\left(\frac{\tau_y h}{\sqrt{M}} \right)_{i+1,j}^{n+1} - \left(\frac{\tau_y h}{\sqrt{M}} \right)_{i,j}^{n+1} \right] \\ &\quad - \frac{M_{i-\frac{1}{2},j}^{n+1}}{\sqrt{M_{i,j}^{n+1}}} \left[\left(\frac{\tau_y h}{\sqrt{M}} \right)_{i,j}^{n+1} - \left(\frac{\tau_y h}{\sqrt{M}} \right)_{i-1,j}^{n+1} \right], \end{aligned} \quad (\text{A.3})$$

where the first term on the right-hand side is

$$\begin{aligned} &\frac{M_{i+\frac{1}{2},j}^{n+1}}{\sqrt{M_{i,j}^{n+1}}} \left[\left(\frac{\tau_y h}{\sqrt{M}} \right)_{i+1,j}^{n+1} - \left(\frac{\tau_y h}{\sqrt{M}} \right)_{i,j}^{n+1} \right] \\ &= \sqrt{M_{i+1,j+1}^{n+1}} \left[\left(\frac{h}{\sqrt{M}} \right)_{i+1,j+1}^{n+1} - \left(\frac{h}{\sqrt{M}} \right)_{i+1,j}^{n+1} \right] \end{aligned}$$

$$\begin{aligned}
& -\sqrt{M_{i+1,j-1}^{n+1}} \left[\left(\frac{h}{\sqrt{M}} \right)_{i+1,j}^{n+1} - \left(\frac{h}{\sqrt{M}} \right)_{i+1,j-1}^{n+1} \right] \\
& -\frac{\sqrt{M_{i+1,j}^{n+1} M_{i,j+1}^{n+1}}}{\sqrt{M_{i,j}^{n+1}}} \left[\left(\frac{h}{\sqrt{M}} \right)_{i,j+1}^{n+1} - \left(\frac{h}{\sqrt{M}} \right)_{i,j}^{n+1} \right] \\
& +\frac{\sqrt{M_{i+1,j}^{n+1} M_{i,j-1}^{n+1}}}{\sqrt{M_{i,j}^{n+1}}} \left[\left(\frac{h}{\sqrt{M}} \right)_{i,j}^{n+1} - \left(\frac{h}{\sqrt{M}} \right)_{i,j-1}^{n+1} \right], \tag{A.4}
\end{aligned}$$

and the second term on the right-hand side is

$$\begin{aligned}
& \frac{M_{i-\frac{1}{2},j}^{n+1}}{\sqrt{M_{i,j}^{n+1}}} \left[\left(\frac{\tau_y h}{\sqrt{M}} \right)_{i,j}^{n+1} - \left(\frac{\tau_y h}{\sqrt{M}} \right)_{i-1,j}^{n+1} \right] \\
& =\frac{\sqrt{M_{i-1,j}^{n+1} M_{i,j+1}^{n+1}}}{\sqrt{M_{i,j}^{n+1}}} \left[\left(\frac{h}{\sqrt{M}} \right)_{i,j+1}^{n+1} - \left(\frac{h}{\sqrt{M}} \right)_{i,j}^{n+1} \right] \\
& -\frac{\sqrt{M_{i-1,j}^{n+1} M_{i,j-1}^{n+1}}}{\sqrt{M_{i,j}^{n+1}}} \left[\left(\frac{h}{\sqrt{M}} \right)_{i,j}^{n+1} - \left(\frac{h}{\sqrt{M}} \right)_{i,j-1}^{n+1} \right] \\
& -\sqrt{M_{i-1,j+1}^{n+1}} \left[\left(\frac{h}{\sqrt{M}} \right)_{i-1,j+1}^{n+1} - \left(\frac{h}{\sqrt{M}} \right)_{i-1,j}^{n+1} \right] \\
& +\sqrt{M_{i-1,j-1}^{n+1}} \left[\left(\frac{h}{\sqrt{M}} \right)_{i-1,j}^{n+1} - \left(\frac{h}{\sqrt{M}} \right)_{i-1,j-1}^{n+1} \right]. \tag{A.5}
\end{aligned}$$

Here, $M_{i-\frac{1}{2},j}^{n+1}$ is approximated by its geometric mean $\sqrt{M_{i-1,j} M_{i,j}}$ and similarly for the other terms at half grid points.

B Truncation errors

B.1 Truncation errors of the concentration equation

Using the Taylor series expansion, we know that

$$\begin{aligned}
\Delta_{+t} v(x,y,t) & = v(x,y,t+\Delta t) - v(x,y,t) \\
& = v_t \Delta t + \frac{1}{2} v_{tt} (\Delta t)^2 + \frac{1}{6} v_{ttt} (\Delta t)^3 + h.o.t., \tag{B.1}
\end{aligned}$$

$$\delta_x v(x,y,t) = v(x + \frac{1}{2} \Delta x, y, t) - v(x - \frac{1}{2} \Delta x, y, t)$$

$$= v_x(\Delta x) + \frac{1}{24}v_{xxx}(\Delta x)^3 + h.o.t., \quad (\text{B.2})$$

$$\begin{aligned} \delta_y v(x, y, t) &= v(x, y + \frac{1}{2}\Delta y, t) - v(x, y - \frac{1}{2}\Delta y, t) \\ &= v_y(\Delta y) + \frac{1}{24}v_{yyy}(\Delta y)^3 + h.o.t., \end{aligned} \quad (\text{B.3})$$

and

$$\begin{aligned} \delta_x^2 v(x, y, t) &= v(x + \Delta x, y, t) - 2v(x, y, t) + v(x - \Delta x, y, t) \\ &= v_{xx}(\Delta x)^2 + \frac{1}{12}v_{xxxx}(\Delta x)^4 + h.o.t., \end{aligned} \quad (\text{B.4})$$

$$\begin{aligned} \delta_y^2 v(x, y, t) &= v(x, y + \Delta y, t) - 2v(x, y, t) + v(x, y - \Delta y, t) \\ &= v_{yy}(\Delta y)^2 + \frac{1}{12}v_{yyyy}(\Delta y)^4 + h.o.t., \end{aligned} \quad (\text{B.5})$$

where h.o.t. stands for higher-order terms. Therefore, the truncation error T_{c_1} of the original five-point scheme (2.1) at $(x, y, t + \Delta t)$:

$$\begin{aligned} T_{c_1}(x, y, t + \Delta t) &:= \varepsilon \frac{\Delta_{-t}c(x, y, t + \Delta t)}{\Delta t} - \frac{\delta_x^2 c(x, y, t + \Delta t)}{(\Delta x)^2} - \frac{\delta_y^2 c(x, y, t + \Delta t)}{(\Delta y)^2} - \rho(x, y, t) \\ &= \varepsilon \frac{c_t \Delta t - \frac{1}{2}c_{tt}(\Delta t)^2 + \frac{1}{6}c_{ttt}(\Delta t)^3}{\Delta t} - \frac{c_{xx}(\Delta x)^2 + \frac{1}{12}c_{xxxx}(\Delta x)^4}{(\Delta x)^2} \\ &\quad - \frac{c_{yy}(\Delta y)^2 + \frac{1}{12}c_{yyyy}(\Delta y)^4}{(\Delta y)^2} - \rho + \rho_t(\Delta t) - \frac{1}{2}\rho_{tt}(\Delta t)^2 + h.o.t. \\ &= (\varepsilon c_t - \Delta c - \rho) - \frac{\varepsilon}{2}c_{tt}(\Delta t) + \frac{\varepsilon}{6}c_{ttt}(\Delta t)^2 - \frac{1}{12}c_{xxxx}(\Delta x)^2 - \frac{1}{12}c_{yyyy}(\Delta y)^2 \\ &\quad + \rho_t(\Delta t) - \frac{1}{2}\rho_{tt}(\Delta t)^2 + h.o.t. \\ &= -\frac{\varepsilon}{2}c_{tt}(\Delta t) + \frac{\varepsilon}{6}c_{ttt}(\Delta t)^2 - \frac{1}{12}c_{xxxx}(\Delta x)^2 - \frac{1}{12}c_{yyyy}(\Delta y)^2 + \rho_t(\Delta t) - \frac{1}{2}\rho_{tt}(\Delta t)^2 + h.o.t. \\ &= O(\Delta t + (\Delta x)^2 + (\Delta y)^2). \end{aligned} \quad (\text{B.6})$$

Similarly, the truncation error T_{c_2} of the ADI scheme (2.2) at $(x, y, t + \Delta t)$:

$$T_{c_2}(x, y, t + \Delta t) = \varepsilon \frac{\Delta_{-t}c}{\Delta t} - \frac{\delta_x^2 c}{(\Delta x)^2} - \frac{\delta_y^2 c}{(\Delta y)^2} + \frac{\Delta t \delta_x^2 \delta_y^2 c}{\varepsilon (\Delta x \Delta y)^2} - \rho(x, y, t). \quad (\text{B.7})$$

We only need to calculate $\delta_x^2 \delta_y^2 c$. By the definitions of δ_x^2 and δ_y^2 , we have

$$\begin{aligned} \delta_x^2 \delta_y^2 c &= \delta_x^2 [c(x, y + \Delta y, t + \Delta t) - 2c(x, y, t + \Delta t) + c(x, y - \Delta y, t + \Delta t)] \\ &= c(x + \Delta x, y + \Delta y, t + \Delta t) - 2c(x, y + \Delta y, t + \Delta t) + c(x - \Delta x, y + \Delta y, t + \Delta t) \end{aligned}$$

$$\begin{aligned}
& -2[c(x+\Delta x, y, t+\Delta t) - 2c(x, y, t+\Delta t) + c(x-\Delta x, y, t+\Delta t)] \\
& + c(x+\Delta x, y-\Delta y, t+\Delta t) - 2c(x, y-\Delta y, t+\Delta t) + c(x-\Delta x, y-\Delta y, t+\Delta t) \\
& = c_{xxyy}(\Delta x \Delta y)^2 + h.o.t..
\end{aligned} \tag{B.8}$$

Therefore, the truncation error T_{c_2} of the ADI scheme (2.2)

$$T_{c_2} = T_{c_1} + \frac{c_{xxyy}}{\varepsilon} \Delta t + h.o.t.. \tag{B.9}$$

B.2 Truncation errors of the density equation

Taking Taylor expansion at $(x, y, t + \Delta t)$, we have

$$M_{i+\frac{1}{2}, j}^{n+1} = M_{i, j}^{n+1} + \frac{1}{2} \partial_x M_{i, j}^{n+1} (\Delta x) + \frac{1}{8} \partial_{xx} M_{i, j}^{n+1} (\Delta x)^2 + h.o.t., \tag{B.10}$$

$$M_{i-\frac{1}{2}, j}^{n+1} = M_{i, j}^{n+1} - \frac{1}{2} \partial_x M_{i, j}^{n+1} (\Delta x) + \frac{1}{8} \partial_{xx} M_{i, j}^{n+1} (\Delta x)^2 + h.o.t., \tag{B.11}$$

$$\left(\frac{h}{\sqrt{M}}\right)_{i+1, j}^{n+1} = \left(\frac{h}{\sqrt{M}}\right)_{i, j}^{n+1} + \partial_x \left(\frac{h}{\sqrt{M}}\right)_{i, j}^{n+1} (\Delta x) + \frac{1}{2} \partial_{xx} \left(\frac{h}{\sqrt{M}}\right)_{i, j}^{n+1} (\Delta x)^2 + h.o.t., \tag{B.12}$$

$$\left(\frac{h}{\sqrt{M}}\right)_{i-1, j}^{n+1} = \left(\frac{h}{\sqrt{M}}\right)_{i, j}^{n+1} - \partial_x \left(\frac{h}{\sqrt{M}}\right)_{i, j}^{n+1} (\Delta x) + \frac{1}{2} \partial_{xx} \left(\frac{h}{\sqrt{M}}\right)_{i, j}^{n+1} (\Delta x)^2 + h.o.t.. \tag{B.13}$$

Therefore, the leading-order Taylor expansion of τ_x is

$$\begin{aligned}
\tau_x h_{i, j}^{n+1} &= \frac{1}{\sqrt{M_{i, j}^{n+1}}} \left[M_{i, j}^{n+1} \partial_{xx} \left(\frac{h}{\sqrt{M}}\right)_{i, j}^{n+1} (\Delta x)^2 + \partial_x M_{i, j}^{n+1} \partial_x \left(\frac{h}{\sqrt{M}}\right)_{i, j}^{n+1} (\Delta x)^2 \right. \\
& \quad \left. + \frac{1}{8} \partial_{xx} M_{i, j}^{n+1} \partial_{xx} \left(\frac{h}{\sqrt{M}}\right)_{i, j}^{n+1} (\Delta x)^4 + h.o.t. \right],
\end{aligned} \tag{B.14}$$

and the corresponding expansion of τ_y is

$$\begin{aligned}
\tau_y h_{i, j}^{n+1} &= \frac{1}{\sqrt{M_{i, j}^{n+1}}} \left[M_{i, j}^{n+1} \partial_{yy} \left(\frac{h}{\sqrt{M}}\right)_{i, j}^{n+1} (\Delta y)^2 + \partial_y M_{i, j}^{n+1} \partial_y \left(\frac{h}{\sqrt{M}}\right)_{i, j}^{n+1} (\Delta y)^2 \right. \\
& \quad \left. + \frac{1}{8} \partial_{yy} M_{i, j}^{n+1} \partial_{yy} \left(\frac{h}{\sqrt{M}}\right)_{i, j}^{n+1} (\Delta y)^4 + h.o.t. \right].
\end{aligned} \tag{B.15}$$

The truncation error of the original scheme (2.5) is

$$T_{\rho_1} := \frac{\Delta_t \rho_{i, j}^{n+1}}{\Delta t} - \frac{\sqrt{M_{i, j}^{n+1}} \tau_x h_{i, j}^{n+1}}{(\Delta x)^2} - \frac{\sqrt{M_{i, j}^{n+1}} \tau_y h_{i, j}^{n+1}}{(\Delta y)^2}$$

$$\begin{aligned}
&= \partial_t \rho_{i,j}^{n+1} - \frac{1}{2} \partial_{tt} \rho_{i,j}^{n+1} (\Delta t) - M_{i,j}^{n+1} \partial_{xx} \left(\frac{h}{\sqrt{M}} \right)_{i,j}^{n+1} - \partial_x M_{i,j}^{n+1} \partial_x \left(\frac{h}{\sqrt{M}} \right)_{i,j}^{n+1} \\
&\quad - \frac{1}{8} \partial_{xx} M_{i,j}^{n+1} \partial_{xx} \left(\frac{h}{\sqrt{M}} \right)_{i,j}^{n+1} (\Delta x)^2 - M_{i,j}^{n+1} \partial_{yy} \left(\frac{h}{\sqrt{M}} \right)_{i,j}^{n+1} - \partial_y M_{i,j}^{n+1} \partial_y \left(\frac{h}{\sqrt{M}} \right)_{i,j}^{n+1} \\
&\quad - \frac{1}{8} \partial_{yy} M_{i,j}^{n+1} \partial_{yy} \left(\frac{h}{\sqrt{M}} \right)_{i,j}^{n+1} (\Delta y)^2 + h.o.t. \\
&= -\frac{1}{2} \partial_{tt} \rho_{i,j}^{n+1} (\Delta t) - \frac{1}{8} \partial_{xx} M_{i,j}^{n+1} \partial_{xx} \left(\frac{h}{\sqrt{M}} \right)_{i,j}^{n+1} (\Delta x)^2 - \frac{1}{8} \partial_{yy} M_{i,j}^{n+1} \partial_{yy} \left(\frac{h}{\sqrt{M}} \right)_{i,j}^{n+1} (\Delta y)^2 + h.o.t. \\
&= O(\Delta t + (\Delta x)^2 + (\Delta y)^2). \tag{B.16}
\end{aligned}$$

In order to calculate the truncation error of the ADI scheme (2.8), we only need to derive the truncation error due to the composite operator $\tau_x \tau_y$. Notice that the coefficients $M_{i+1,j+1}^{n+1}, M_{i+1,j-1}^{n+1}, M_{i-1,j}^{n+1}, M_{i,j+1}^{n+1}, M_{i,j-1}^{n+1}$ converge to $M_{i,j}^{n+1}$ when Δx and Δy tend to 0. Therefore, the composite operator $\tau_x \tau_y$ (A.3) can be simplified to

$$\begin{aligned}
\tau_x \tau_y h_{i,j}^{n+1} &= \frac{1}{\sqrt{M_{i,j}^{n+1}}} \delta_x \left[M_{i,j}^{n+1} \delta_x \left(\frac{\tau_y h}{\sqrt{M}} \right)_{i,j}^{n+1} \right] \\
&= \frac{M_{i+\frac{1}{2},j}^{n+1}}{\sqrt{M_{i,j}^{n+1}}} \left[\left(\frac{\tau_y h}{\sqrt{M}} \right)_{i+1,j}^{n+1} - \left(\frac{\tau_y h}{\sqrt{M}} \right)_{i,j}^{n+1} \right] \\
&\quad - \frac{M_{i-\frac{1}{2},j}^{n+1}}{\sqrt{M_{i,j}^{n+1}}} \left[\left(\frac{\tau_y h}{\sqrt{M}} \right)_{i,j}^{n+1} - \left(\frac{\tau_y h}{\sqrt{M}} \right)_{i-1,j}^{n+1} \right] \\
&= \sqrt{M_{i,j}^{n+1}} \left\{ \left[\left(\frac{h}{\sqrt{M}} \right)_{i+1,j+1}^{n+1} - \left(\frac{h}{\sqrt{M}} \right)_{i+1,j}^{n+1} \right] - \left[\left(\frac{h}{\sqrt{M}} \right)_{i+1,j}^{n+1} - \left(\frac{h}{\sqrt{M}} \right)_{i+1,j-1}^{n+1} \right] \right. \\
&\quad \left. - \left[\left(\frac{h}{\sqrt{M}} \right)_{i,j+1}^{n+1} - \left(\frac{h}{\sqrt{M}} \right)_{i,j}^{n+1} \right] + \left[\left(\frac{h}{\sqrt{M}} \right)_{i,j}^{n+1} - \left(\frac{h}{\sqrt{M}} \right)_{i,j-1}^{n+1} \right] \right\} \\
&\quad + \sqrt{M_{i,j}^{n+1}} \left\{ \left[\left(\frac{h}{\sqrt{M}} \right)_{i,j+1}^{n+1} - \left(\frac{h}{\sqrt{M}} \right)_{i,j}^{n+1} \right] - \left[\left(\frac{h}{\sqrt{M}} \right)_{i,j}^{n+1} - \left(\frac{h}{\sqrt{M}} \right)_{i,j-1}^{n+1} \right] \right. \\
&\quad \left. - \left[\left(\frac{h}{\sqrt{M}} \right)_{i-1,j+1}^{n+1} - \left(\frac{h}{\sqrt{M}} \right)_{i-1,j}^{n+1} \right] + \left[\left(\frac{h}{\sqrt{M}} \right)_{i-1,j}^{n+1} - \left(\frac{h}{\sqrt{M}} \right)_{i-1,j-1}^{n+1} \right] \right\} + h.o.t. \\
&= O((\Delta x \Delta y)^2). \tag{B.17}
\end{aligned}$$

Therefore, the truncation error due to the composite operator $\tau_x \tau_y$ is

$$\tau_x \tau_y v = O((\Delta x \Delta y)^2). \tag{B.18}$$

In the end, the truncation error of (2.8) is

$$T_{\rho_2} = T_{\rho_1} + O(\Delta t). \quad (\text{B.19})$$